Lib.

DEC 17 1946

THE JOURNAL OF CHEMICAL PHYSICS

VOLUME 14 NUMBER 12

DECEMBER, 1946

Published by the

AMERICAN INSTITUTE OF PHYSICS

Incorporated

LANCASTER, PA., AND NEW YORK, N. Y.

THE JOURNAL
OF
CHEMICAL PHYSICS

VOLUME 14, NUMBER 12 DECEMBER, 1946

Mass Spectrometric Study of CH_3D. Dissociation Probabilities of C—H and C—D Bonds by Electron Impact

MARJORIE W. EVANS, NORMAN BAUER, AND J. Y. BEACH
California Research Corporation, Richmond Laboratories, Richmond, California

(Received June 27, 1946)

A pure sample of CH_3D has been prepared and studied in the mass spectrometer. The mass spectrum of CH_3D cannot be predicted from that of CH_4 by assuming complete similarity between H and D (except mass). More information has been obtained on the difference in behavior of H and D on electron impact previously noticed by Delfosse and Hipple for $C_2H_2D_2$. There is a difference in dissociation probability of C−H and C−D bonds which is approximately constant for several ionization processes and over a considerable range in electron energy. In addition to this there is a difference in behavior of H atoms in CH_4 and H atoms in CH_3D. In order to account for the mass spectrum of CH_3D in terms of the mass spectrum of CH_4 both these effects must be taken into consideration. Re-examination of the data of Delfosse and Hipple points not only to the difference between H and D atoms in $C_2H_2D_2$, but also to a difference in behavior of H atoms in C_2H_4 and H atoms in $C_2H_2D_2$.

INTRODUCTION

DELFOSSE and Hipple,[1] in a mass spectrometric study of di-deutero-ethylene, *cis* and *trans*, showed that upon dissociation by electron impact the splitting of the C−H bond is favored over the splitting of the C−D bond. In accounting for ions of high mass, which are formed by breaking C−H and C−D bonds only, they obtained a factor of 0.3 for the relative probability of dissociation of a C−D and C−H bond. For ions in the low mass region, formed by breaking the carbon-carbon bond in addition to carbon-hydrogen bonds, a factor of 0.5 was obtained. They also compared the relative abundance of corresponding ions in C_2H_4 and $C_2H_2D_2$, and found that they were nearly the same with the exception of the $(C_2H_3^+)$ type. We believe this exception to be significant.

[1] J. Delfosse and J. A. Hipple, Phys. Rev. **54**, 1060 (1938).

In an effort to reduce the complicating factors of interpretation to a minimum we have prepared the simpler molecule mono-deutero-methane and obtained its mass spectrum. This spectrum has been examined with a view to determining if the selective process observed for di-deutero-ethylene is a general phenomenon. Secondly, the spectrum for CH_3D has been compared to that for CH_4 in an attempt to discover the reason for the anomalous behavior of the $(C_2H_3^+)$ type ion from $C_2H_2D_2$.

We obtained spectra for a series of electron energies ranging from 55 volts down to the region of the appearance potentials of the several ions. At the lower energies the effect of ions formed by the liberation of more than one hydrogen type atom is reduced to a minimum. Furthermore, the generality of the phenomenon of selective splitting is tested over a wide range of impact energies.

TABLE I. Relative intensities of ions of given m/e for CH_3D and CH_4 produced by 55-volt electrons.

Ions	CH_3D	CH_4
(CH_4^+)		100.0
(CH_3D^+)	100.0	
(CH_2D^+)	75.6 ±0.6	
$(CH_3^+ + CHD^+)$	22.4 ±0.1	82.6
$(CH_2^+ + CD^+)$	9.41±0.10	17.0
(CH^+)	5.20±0.07	8.19
(C^+)	2.41±0.03	2.35
(HD^+)	0.12	
$(H_2^+ + D^+)$	0.74±0.02	0.35
(H^+)	4.60±0.10	5.45

Finally, it is of interest to test the existence of the effect for the splitting off of H^+ and D^+ ions as well as of H and D neutral atoms.

EXPERIMENTAL

The purity of the CH_3D, particularly with regard to the presence of CH_4, was of utmost importance. The compound was prepared by the reaction of D_2O with the Grignard reagent methyl magnesium iodide in diethyl ether. The total volume of the reaction unit was 75 cc. Hence, the relative amount of H_2O remaining on the glass after forty-eight hours of heating at 100°C should be negligible in comparison to the one cc of D_2O used. In order to test possible water contamination during assembly of apparatus and transfer of reagents the vapor in equilibrium with the Grignard solution was withdrawn at reduced pressure and analyzed for CH_4. Within the limit of detection (0.1 percent) no CH_4 was found.

The product CH_3D was fractionated from the ether until no ether peaks were observed in the mass spectrum. The final product showed no m/e peak greater than 17.

The D_2O was analyzed both by density measurements and by conversion to D_2 with subsequent analysis in the mass spectrometer. Both analyses showed that the sample was 99 percent D_2O or better.

The mass spectrometer was the Consolidated Engineering Corporation instrument.[2] The gas pressures used were low enough to insure that only the primary products of electron impact were observed.

[2] H. W. Washburn, H. F. Wiley, and S. M. Rock, Ind. Eng. Chem. Anal. Ed. **15**, 541 (1943).

For the ionizing efficiency curves the nominal values of electron energy, as set on the instrument voltmeter to ±0.3 volt, were corrected to include the effect of ion draw-out or pusher voltages. Although for each different m/e the ionizing electrons acquire different amounts of energy from the pusher voltage because the pusher voltage is proportionate to the ion accelerating voltage, the proper correction at each m/e can be derived easily from calibrations with a gas of known appearance potential. By calibrations with argon, the ratio between electron energy correction and ion accelerating voltage was determined with an accuracy of about 5 percent, allowing the assignment of electron energies to within 0.5 volt. The difference between the appearance potential of CH_3D ions and that of CH_4 ions is influenced only slightly (~0.1 volt) by the probable error in the pusher voltage corrections. Decrease of gas pressure during the measurement of ion intensity as a function of electron energy was minimized by the use of a large sample reservoir (15 liters), and a small correction for this decrease was made.

Three samples of CH_3D were prepared, and satisfactory agreement of the spectra was obtained. For purposes of comparison a sample of CH_4 was prepared in the same manner.

RESULTS

The average values obtained for the relative ion intensities for CH_3D are listed in Table I, together with those obtained for CH_4 under similar instrument conditions. The ion intensity per unit pressure is the same for CH_3D^+ and CH_4^+, within 1 percent.

A simple relationship might be expected between the mass spectra of CH_3D and CH_4. One can try to predict the spectrum of CH_3D by

TABLE II. Spectrum of CH_3D predicted from that of CH_4 assuming identical behavior of H and D.

Ion	CH_4 spectrum	Predict CH_3D
CH_3D^+		100.0
CH_4^+	100.0	
CH_2D^+		62.0
CH_3^+	82.6	20.6
CHD^+		8.5
CH_2^+	17.0	8.5
CD^+		2.04
CH^+	8.19	6.15

assuming (1) that H and D atoms behave in identical fashion in CH_3D, and (2) that H's in CH_3D and CH_4 are likewise identical. It is furthermore reasonable to assign ion intensities for the CH_3D spectrum by applying simple statistics to the CH_4 spectrum; e.g. (CH_3^+ from CH_3D) = $\frac{1}{4}$(CH_3^+ from CH_4). In this way the values given in Table II are obtained. In Table III the values of column three, Table II, are summed in order to compare the predicted intensities of ions for a given m/e with the intensities actually observed. The disagreement in Table III shows that the above simple approach is not adequate.

We proceed to test our first assumption, namely, that H and D are identical in deutero-methane. With this assumption we shall find that the apportioning of intensities observed at each m/e to individual ions of the CH_3D spectrum results in internal inconsistencies, as shown below. Equations (1)–(3) express the relationships to be tested.

$$(CH_2D^+) = 3(CH_3^+), \tag{1}$$

$$3(CD^+) = (CH^+), \tag{2}$$

$$(CHD^+) = (CH_2^+). \tag{3}$$

Substituting the appropriate values of CH_3D peaks (Table I), we have:

$$(CHD^+) = 22.4 - (CH_3^+) = 22.4 - 75.6/3 = -2.8$$

and

$$(CH_2^+) = 9.41 - (CD^+) = 9.41 - 5.20/3 = 7.68.$$

Consequently $(CHD^+) \neq (CH_2^+)$ and assumption (1) is therefore incorrect. We conclude that the same selectivity of splitting shown with $C_2H_2D_2$ is exhibited here.

It should be possible to calculate the relative probability of breaking a C–D bond, and the correlative factor can be defined as follows:

$$\pi_D = \frac{\text{probability of D leaving } CH_3D}{\text{probability of individual H leaving } CH_3D}.$$

We make the simplifying assumption that π_D is constant for the formation of all types of ions from CH_3D. Equations (1)–(3) are now written

$$\left.\begin{aligned} 3(CH_3^+) &= \pi_D(CH_2D^+) \\ \text{or} \qquad (CHD^+) &= 22.4 - 75.6\pi_D/3, \end{aligned}\right\} \tag{4}$$

$$\left.\begin{aligned} (CH^+) &= 3\pi_D(CD^+) \\ \text{or} \qquad (CH_2^+) &= 9.41 - 5.20/3\pi_D, \end{aligned}\right\} \tag{5}$$

$$(CH_2^+) = \pi_D(CHD^+). \tag{6}$$

Solving, we find that π_D for deutero-methane when 55-volt electrons are used is 0.38, a figure with which the Delfosse and Hipple value of 0.3–0.5 compares reasonably well.

The effect of subtraction from the ion intensities of the contribution of 1 percent CH_4 due to possible H_2O in the D_2O is to lower π_D to 0.37, which is within the experimental error.

We can also make an estimate of the numerical value of the π_D^+ factor, which will express the relative ease of breaking C–D and C–H bonds to form D^+ and H^+ ions.

We can place an upper limit on this value by assuming that no H_2^+ is formed in the ionization chamber, thus attributing the entire 2 peak (0.74) to the D^+ ion, and finding

$$\pi_D^+(\max) = \frac{3(0.74)}{4.60} = 0.48.$$

The true value will be smaller than 0.48, for some H_2^+ is undoubtedly formed, and this would make the intensity attributable to D^+ smaller.

TABLE III. Observed spectrum of CH_3D compared with predicted spectrum assuming identical behavior of H and D.

m/e	Observed	Predicted from CH_4
16	75.6	62.0
15	22.4	29.1
14	9.41	10.54
13	5.20	6.15

TABLE IV. Relative intensities for individual ions of CH_3D; predictions from CH_4 using $\pi_D = 0.38$.

Ion	"Observed" CH_3D	Predict CH_3D
CH_3D^+	100.0	100.0
CH_2D^+	75.6	62.0
CH_3^+	9.6	7.8
CHD^+	12.8	8.5
CH_2^+	4.85	3.2
CD^+	4.56	2.05
CH^+	5.20	2.34

TABLE V. "Observed" and predicted CH_3D spectra assuming 12 percent methane impurity.

Ion	CH_3D "Observed"	Predict from CH_4 $\pi_D=0.25$
CH_2D^+	(62.0)	(62.0)
CH_3^+	5.18	5.15
CHD^+	6.02	8.5
CH_2^+	1.52	2.12
CD^+	5.48	2.05
CH^+	4.12	1.54

The CH_4 pattern, for example, shows an (H_2^+) peak of 0.35. If one-half as much (H_2^+) is formed from CH_3D as from CH_4,

$$\pi_D^+=\frac{3}{4.60}(0.74-0.5\times 0.35)=0.37.$$

A check on this second value is to assume that the sum of the corresponding ions H_2^+ and HD^+ in CH_3D equals H_2^+ in CH_4. Then

$$H_2^+(CH_3D)=0.35-0.12=0.23$$

and

$$\pi_D^+=\frac{3}{4.60}(0.74-0.23)=0.33.$$

The best that can be said is that π_D^+ is certainly less than 0.5 and probably greater than 0.3, an interesting result in view of the value $\pi_D=0.38$.

We can now return to the problem of finding a correlation between the CH_3D and CH_4 spectra, correcting our first assumption by introducing π_D in the following way. With the known value of π_D applied to Eqs. (4)–(6), the observed peak heights of CH_3D (Table I) can be broken down into "observed" contributions due to individual ions, shown in column two of Table IV. Similarly, the value of π_D is used to predict (Table IV, column three) the individual ion intensities of CH_3D from the CH_4 spectrum; e.g., $(CH_3^+$ from $CH_3D)=\pi_D/4(CH_3^+$ from $CH_4)$.

The predictions and observations are still at wide variance, though all differences are now in the same direction. The first thought is to attribute the disagreement to a CH_4 impurity, despite precautions taken against this occurrence. This explanation cannot suffice even by attributing to methane all of the discrepancy observed for the 16 peak, which amounts to 75.6−62.0 =13.6 units. This amount of CH_4 (12 percent) would necessitate a corresponding correction to the CH_3D spectrum and would cause π_D to be lowered from 0.38 to 0.25. Table V compares the predicted and "observed" spectra on the basis of $\pi_D=0.25$, and shows that this extreme correction fails to remove all the discrepancies. Furthermore, the fact that the ion intensity per unit pressure was found to be equal within 1 percent for CH_4^+ and CH_3D^+ supports the expectation that both the CH_4 and the CH_3D preparations contained no more than about 1 percent impurity. It is reasonable, therefore, to regard the differences indicated in Table IV as real and caused by the incorrectness of our second original assumption, namely, that H's in CH_3D and CH_4 are identical. In fact, we shall see that these differences mean that the presence of the D atom in the molecule causes the H atom to be removed more easily from CH_3D than from CH_4.

TABLE VI. Comparison of intensities of corresponding ions of CH_3D and CH_4.

Ion type	CH_3D	CH_4
CX_4^+	100.0	100.0
CX_3^+	85.2	82.6
CX_2^+	17.65	17.0
CX^+	9.76	8.19
C^+	2.41	2.35

We define a new quantity Γ_H.

$$\Gamma_H=\frac{\text{probability of individual H leaving } CH_3D}{\text{probability of individual H leaving } CH_4}.$$

TABLE VII. Relative ion intensities for C_2H_4 and $C_2H_2D_2$.

Ion	Observed $C_2H_2D_2$[a]	Observed C_2H_4[a]	Predict $C_2H_2D_2$ $\pi_D=1$	Predict $C_2H_2D_2$ $\pi_D=0.33$	Γ_H $\pi_D=0.33$
$C_2H_2D_2^+$	100	100	100	100	
$C_2H_2D^+$	11	60	30	10	1.13
$C_2HD_2^+$	34		30	30	
$C_2D_2^+$	24		9.5	9.5	
C_2HD^+	32.5		38	12.6	1.59
$C_2H_2^+$	2.6	57	9.5	1.03	
C_2D^+	8.2		4.8	1.59	1.73
C_2H^+	2.7	9.6	4.8	0.53	

[a] See reference 1 in text.

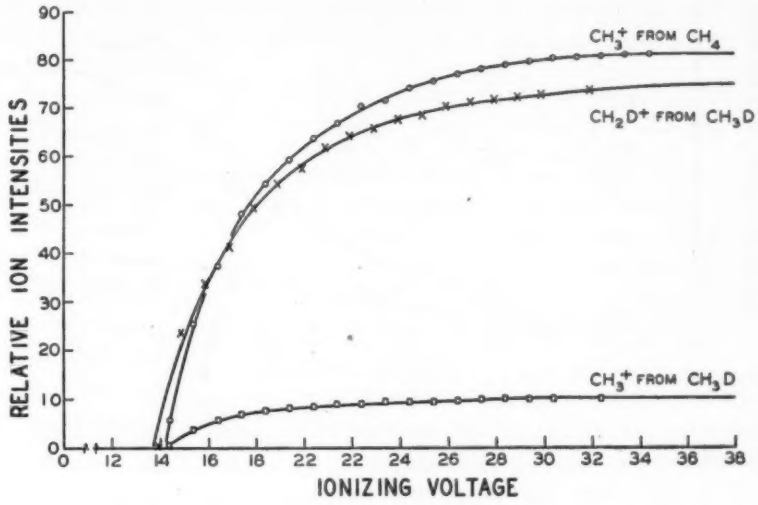

FIG. 1. Voltage of the ionizing electrons *versus* relative ion intensities of CX_3^+ type ions. The CH_3^+ ion from methane is relative to the CH_4^+ ion; CH_3^+ and CH_2D^+ ions from monodeutero-methane are relative to the CH_3D^+ ion. Ionizing current is constant.

The subscript *DM* will refer to the compound CH_3D, *M* to CH_4. The expression $(CH_2D^+)_M$ refers to a hypothetical ion formed from CH_3D in which H and D both behave exactly like H in CH_4.

$$(CH_2D^+)_M = 3/4(CH_3^+)_M,$$

$$\Gamma_H(CH_2D^+)_M = (CH_2D^+)_{DM},$$

$$\Gamma_H = 4/3 \times \frac{(CH_2D^+)_{DM}}{(CH_3^+)_M}$$

$$= 4/3 \times 75.6/82.6 = 1.22$$

For the ions $(CH_2^+)_{DM}$ and $(CHD^+)_{DM}$

$$\Gamma_H^2(CHD^+)_M = (CHD^+)_{DM},$$

$$\Gamma_H^2 = \frac{2(CHD^+)_{DM}}{(CH_2^+)_M} = \frac{2 \times 12.8}{17.0} = 1.507,$$

$$\Gamma_H = 1.23.$$

TABLE VIII. π_D for CH_3D over a range of electron energies.

Electron energy (volts)	π_D	Electron energy (volts)	π_D
55	0.38	23	0.41
32	0.40	22	0.40
30	0.40	21	0.42
29	0.40	20	0.42
28	0.41	19	0.43
27	0.40	18	0.44
26	0.40	17	0.44–0.46
25	0.39	16	0.35–0.47
24	0.40	15	0.69–0.43

For the ions $(CH^+)_{DM}$ and $(CD^+)_{DM}$

$$\Gamma_H^3(CD^+)_M = (CD^+)_{DM},$$

$$\Gamma_H = \left(\frac{4 \times 4.56}{8.19}\right)^{\frac{1}{3}} = 1.31.$$

It is apparent that two effects exist. The first is the "π effect," which measures the difference in activity of an H and a D on the same carbon atom. This amounts to a factor of about 2.6. The second is the "Γ effect," which is a specific activation of H atoms on CH_3D over H on CH_4. The hydrogen atoms on deutero-methane are removed 20 percent–30 percent more easily than those on ordinary methane.

The fact that the sums of the CH_3D corresponding ions agree fairly well with the corresponding ions of CH_4 (Table VI) appears to be fortuitous and the result of two opposing effects which in large part cancel each other.

Delfosse and Hipple found similar rough agreement of intensities of corresponding ions of $C_2H_2D_2$ and C_2H_4 with the exception of the ion type $(C_2X_3^+)$. In this connection we have reexamined their data to see if this discrepancy can be removed by including a gamma effect.

Table VII shows the C_2H_4 and $C_2H_2D_2$ spectra, with the spectrum for $C_2H_2D_2$ predicted from C_2H_4 using $\pi_D = 1$ and $\pi_D = 0.33$. The last column gives the values of Γ_H which we have calculated for different ion types of the molecule. The values do not show the same constancy observed in the case of CH_3D, but it is apparent that there

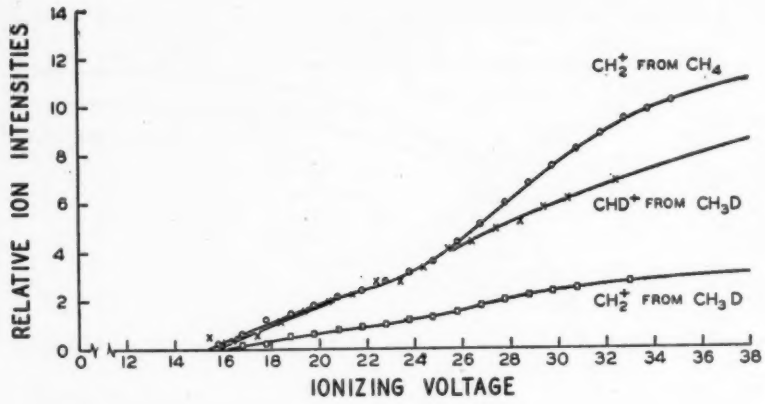

FIG. 2. Voltage of the ionizing electrons *versus* relative ion intensities of CX_2^+ type ions. The CH_2^+ ion from methane is relative to the CH_4^+ ion; CH_2^+ and CHD^+ ions from mono-deutero-methane are relative to the CH_3D^+ ion. Ionizing current is constant.

does exist an activating influence on H, assuming the absence of C_2H_4 in the sample.

The spectrum for mono-deutero-ethane has been tentatively examined and similar effects are indicated.

In addition to the spectra of CH_3D and CH_4 for 55-volt electrons, spectra for electron energies ranging from 14 to 32 volts have been obtained. π_D was calculated for each of these voltages, with results as shown in Table VIII. Values for π_D below 18 volts are not precise since the ion currents at these low voltages are small and error is correspondingly greater. The pairs of π_D values at 17, 16, and 15 volts are those calculated from two spectra.

π_D remains remarkably constant (0.40 ± 0.01) for the wide range of electron impact energies between 55 and 22 volts; at lower energies the value increases slightly. It is below about 23 volts that the ions CH^+ and CD^+ are no longer observed, as may be seen in Fig. 3. This suggests that our assumption of the constancy of π_D for formation of all types of ions is not completely justified, and that π_D is somewhat higher for the heavier ions.

Ion intensities of individual ions from CH_3D have been calculated from π_D for each voltage with the result that ionizing efficiency curves may be drawn for each ion. In Fig. 1 the curves for the ions (CH_2D^+) and (CH_3^+) from CH_3D and (CH_3^+) from CH_4 are plotted. Figures 2 and 3 are similar curves for the (CX_2^+) and (CX^+) type, respectively.

The double inflection of the curve for (CH_2^+) from CH_4 in Fig. 2 is caused by the fact that the (CH_2^+) ion is formed in two different ways, as shown by Smith.[3] The appearance potentials of the ions from CH_4 agreed within experimental error with the values given by Smith. The curves show that within the experimental uncertainty of ± 0.5 volts the corresponding ions of the two molecules have the same appearance potentials.

The existence of these effects suggest that caution must be used in analyzing for deuterium isotope concentration with the mass spectrometer. In some cases it may be necessary to obtain the spectrum for the pure tagged compound before the analysis of a mixture of tagged and untagged molecules can be performed. For example, if the predicted pattern of Table II is used instead of the correct pattern of Table I for prediction of concentration of CH_3D in a mixture of CH_3D and CH_4, considerable error may be made. The analysis for CH_3D in a 50–50 mixture will be in error by 14 percent of the

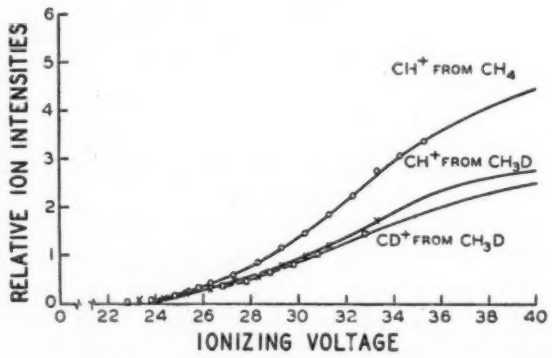

FIG. 3. Voltage of the ionizing electron *versus* relative ion intensities of CX^+ type ions. The CH^+ ion from methane is relative to the CH_4^+ ion; CH^+ and CD^+ ions from mono-deutero-methane are relative to the CH_3D^+ ion. Ionizing current is constant.

[3] L. G. Smith, Phys. Rev. **51**, 263 (1937).

CH_3D present. However, parent ions (i.e., those formed by the removal of an electron from the parent molecule) of corresponding molecules have shown the same intensity per unit pressure in all cases observed. Therefore, if it is possible to use only the parent ions as measures of concentration, it should not be necessary to examine the spectrum of the pure isotope-substituted compound.

No detailed explanation has been developed for these effects. However, the π and Γ deduced here give definite information about a specific type of reacting system. It seems reasonable to suppose that they can be of considerable assistance in extending present methods of making rate and reaction mechanism calculations.

Note added in proof: Since this manuscript was submitted for publication, it has come to our attention (through Dr. D. P. Stevenson) that Bleakney, Condon, and Smith, J. Phys. Chem. **41**, 197 (1937), account for the difference in ratio of atomic to molecular ions between H_2 and D_2 on the basis of the difference in zero point amplitudes of vibration and the Franck-Condon principle. This doubtless provides the basis for the explanation of the effects reported above. It seems certain that if sufficiently accurate information were available on ground normal vibrational wave functions and on excited electronic states it would be possible to calculate the π and the Γ effect for CH_3D and other deuterium containing molecules.

THE JOURNAL OF CHEMICAL PHYSICS VOLUME 14, NUMBER 12 DECEMBER, 1946

The Mercury Photo-Sensitized Reaction Between Hydrogen and Oxygen[1]

DAVID H. VOLMAN
Noyes Chemical Laboratory, University of Illinois, Urbana, Illinois and
Division of Chemistry, College of Agriculture, University of California, Davis, California

(Received August 26, 1946)

The mercury sensitized reaction between hydrogen and oxygen in a flowing system was studied. The quantum yield of the reaction was found to be less than unity, and no evidence of a chain reaction at 40° was found. Hydrogen peroxide was the principal product, and yields of peroxide above 90 percent were found for many of the experiments. It was shown that in the gas phase reaction between ozone and hydrogen peroxide, water was rapidly formed. The yield of product was found to increase with increasing oxygen flow rate, with increasing total flow rate for a fixed hydrogen to oxygen ratio, and to increase and then decrease with increasing hydrogen to oxygen ratio. The reaction scheme proposed is

$$\mathrm{Hg}+h\nu\rightarrow\mathrm{Hg}^*,$$
$$\mathrm{Hg}^*+\mathrm{H_2}\rightarrow\mathrm{H}+\mathrm{H}+\mathrm{Hg},$$
$$\mathrm{Hg}^*+\mathrm{O_2}\rightarrow\mathrm{O_2}+\mathrm{Hg},$$
$$\mathrm{H}+\mathrm{O_2}\rightarrow\mathrm{HO_2},$$
$$\mathrm{H}+\mathrm{M}\rightarrow\mathrm{HM},$$
$$\mathrm{HM}+\mathrm{HM}\rightarrow\mathrm{H_2}+\mathrm{M},$$
$$\mathrm{HO_2}+\mathrm{HO_2}\rightarrow\mathrm{H_2O_2}+\mathrm{O_2}.$$

This leads to the rate equation,

$$\frac{d(\mathrm{H_2O_2})}{dt}=\frac{k_3/k_4''(\mathrm{O_2})}{k_3/k_4''(\mathrm{O_2})+1}\,\frac{I_a k_1/k_2(\mathrm{H_2})}{k_1/k_2(\mathrm{H_2})+(\mathrm{O_2})},$$

using the flow rates of hydrogen and oxygen. k_1/k_2 is the ratio of quenching efficiencies of hydrogen and oxygen for activated mercury or 1.62. k_3/k_4'' is taken equal to 1.2×10^{-3}.

INTRODUCTION

IT has been shown by Coehn and Grote[2] that hydrogen peroxide could be detected among the reaction products if a mixture of hydrogen and oxygen was passed rapidly through an irradiated quartz vessel. In a static experiment or when using low rates of flow no peroxide was detected. That hydrogen and oxygen can react in the presence of photo-activated mercury atoms at room temperature was first established by Dickinson.[3] Later it was demonstrated by Marshall[4] that, in a flowing system, hydrogen peroxide was formed and that the quantum yield of the reaction was about 6.6. This value was later corrected to about 2.5.[5] Bates and

[1] The experimental work reported herein was carried out at the University of Illinois, and this report is based on work performed for the O.S.R.D. under Contract No. OEM-sr-1452.

[2] G. K. Rollefson and M. Burton, *Photochemistry and the Mechanism of Chemical Reactions* (Prentice-Hall, Inc., New York, 1939), p. 173.

[3] R. G. Dickinson, Proc. Nat. Acad. Sci. **10**, 409 (1924).

[4] A. L. Marshall, J. Phys. Chem. **30**, 1078 (1926).

[5] A. L. Marshall, J. Am. Chem. Soc. **54**, 4460 (1932).

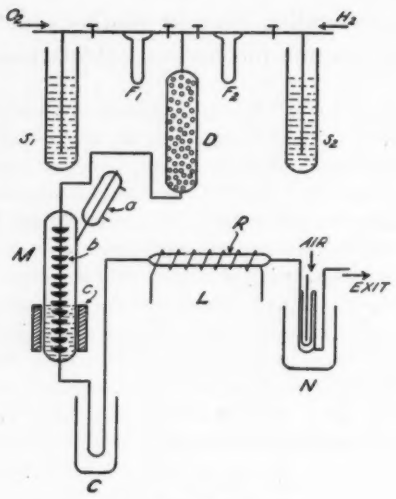

FIG. 1. Gas flow system.

Taylor[6] and Bates and Salley[7] demonstrated that under suitable flow conditions, and with a proper ratio of hydrogen and oxygen, hydrogen peroxide was the principal reaction product. Frankenburger and Klinkhardt[8] report results at variance with those of Marshall and Bates and co-workers in that they found a quantum yield of only about unity and considerable water in the reaction products.

The data existing in 1933 were considered critically by Bates[9] who advanced the following reaction scheme:

$$\mathrm{Hg}+h\nu\rightarrow\mathrm{Hg}^* \qquad I_a \qquad (1)$$

$$\mathrm{Hg}^*+\mathrm{H_2}\rightarrow\mathrm{H}+\mathrm{H}+\mathrm{Hg} \qquad k_1 \qquad (2)$$

$$\mathrm{Hg}^*+\mathrm{O_2}\rightarrow\mathrm{O_2}+\mathrm{Hg} \qquad k_2 \qquad (3)$$

$$\mathrm{H}+\mathrm{O_2}\rightarrow\mathrm{HO_2} \qquad k_3 \qquad (4)$$

$$\mathrm{HO_2}+\mathrm{H_2}\rightarrow\mathrm{H_2O_2}+\mathrm{H} \qquad k_4 \qquad (5)$$

$$\mathrm{HO_2}+\mathrm{HO_2}\rightarrow\mathrm{H_2O_2}+\mathrm{O_2}. \qquad k_5 \qquad (6)$$

This chain mechanism allows quantum yields of greater than unity and predicts that hydrogen peroxide is the sole product. The mechanism is based on assumptions in regard to the incident intensity in the experiments of the earlier investigations, and explains the difference in the quantum yields reported by Frankenburger and Klinkhardt, and by Marshall quantitatively by use of the differences in incident intensity. The quantum yield given by Frankenburger and Klinkhardt is based on the use of monochloroacetic acid as an actinometer and the values of the quantum yield for the photo-hydrolysis reaction given by Rudberg.[10] However, more recent work[11] has established a value somewhat less than that reported by Rudberg. These newer data indicate that the values given by Frankenburger and Klinkhardt should be lowered, probably well below unity. These considerations, especially the uncertainties in quantum yield, throw some question on the necessity for postulating a chain mechanism. In this paper a re-investigation of some of the experimental work and a revised interpretation of the reaction mechanism are presented.

EXPERIMENTAL

Apparatus

The apparatus used to study the photochemical reaction is shown diagrammatically in Fig. 1. Tank oxygen and hydrogen were measured by calibrated flowmeters, F_1 and F_2. The hydrogen was made oxygen free by prior passage over heated copper. Constant flow was maintained by allowing a small amount of gas to escape through the constant head stabilizers, S_1 and S_2. The gases were mixed and dried in D over magnesium perchlorate. The mixture of gases then passed through the mercury saturator $M-C$. From here they were brought to 20° in the water bath, C, and then passed through the quartz reaction tube R at 40°. The reaction tube was enclosed by a mercury resonance lamp of the rare gas-mercury discharge type which was in the form of a helix 25 mm in diameter and 200 mm long, L. Condensable product was collected in the liquid air trap N.

To insure a constant pressure of mercury vapor it was decided to saturate the gas stream at some temperature below the reaction temperature so that there would be no condensation of mercury vapor in the reaction tube. Mercury is held in cuplike depressions, b. The electrical

[6] J. R. Bates and H. S. Taylor, J. Am. Chem. Soc. **49**, 2438 (1927).
[7] J. R. Bates and D. J. Salley, J. Am. Chem. Soc. **55**, 110 (1933).
[8] W. Frankenburger and H. Klinkhardt, Zeits. f. physik. Chemie **B15**, 421 (1932).
[9] J. R. Bates, J. Chem. Phys. **1**, 457 (1933).
[10] E. Rudberg, Leitz. f. Physik **24**, 247 (1924).
[11] R. N. Smith, P. A. Leighton, and W. G. Leighton, J. Am. Chem. Soc. **61**, 2299 (1939).

heater, *c*, and the water-jacketed condenser, *a*, maintain boiling water in the space surrounding the cups. The gas stream is very likely only partially saturated at 100° in passing over the mercury containers. However, reducing the temperature to 20° in *C* insures saturation at this temperature, and a constant pressure of mercury vapor is obtained.

It is difficult to trap out a small quantity of condensable gas from a large quantity of non-condensable gas at atmospheric pressure. Using liquid air or dry ice as the refrigerant, fogs are readily formed and are carried through the trap. In the case where water is the condensable gas, a characteristic snow may sometimes be seen in the effluent gas stream. Bates and Salley[7] in experiments similar to ours found that it was necessary to use several U type or bubbler type traps in series in order to insure capturing almost all of the condensable fraction. In our experiments it was found that it was not possible to collect all of the product in an ordinary bubbler type trap, and a trap of rather unique design was constructed. A stream of room temperature air enters the well as shown. This sets up a large temperature gradient in the annular space through which the gases are forced to pass. The space is only about 1 mm thick. The arrangement is effective in preventing or dissipating water or hydrogen fogs, and the entire condensable product is collected on the cold surface of the outer glass cylinder.

Analytical Procedure

Although considerable work has been carried out to establish the fact that hydrogen peroxide could be produced in yields in the neighborhood of 85 percent or even higher, the evidence did not appear to be conclusive. Bates and Salley have described their technique in considerable detail. At the end of an experiment, the trap was allowed to come to room temperature, weighed, and then titrated. Since the gas mixture was usually about 10 volumes of hydrogen to 1 of oxygen, the difference between the weight of this gas mixture and the weight of an equal volume of air would be an important factor. In this study it was found that diffusion was too slow to allow for replacement of the gas mixture by air. However, dry air could be used to flush out the trap while the trap was still very cold so that none of the condensed product was lost. The most satisfactory technique was to turn off the hydrogen gas at the end of an experiment and then continue the flow of oxygen until all of the hydrogen was replaced. A relatively small correction for the difference in density of oxygen and air could then be made. This procedure served a dual role in that it eliminated the danger of leaving an explosive mixture in the reaction system. The peroxide content was then determined by titration with potassium permanganate.

Reaction with Mercury

In many of the experiments, an oxide deposit was observable in the region just past the illumination zone. In all experiments, however, the major part of the mercury was collected in the trap along with the condensable products. This mercury appeared black until the trap was allowed to warm up, when it assumed an appearance characteristic of mercuric oxide. Bates and Salley have observed similar effects. It was important to know whether the reaction resulted in catalytic decomposition of the peroxide.

In experiments in which solutions of 30 percent hydrogen peroxide were mixed with mercury, mercuric oxide was forned and only stoichiometric amounts of peroxide were used up; oxygen gas is liberated in the reaction. Hydrogen peroxide was found to decompose only very slightly more rapidly over mercuric oxide than it does ordinarily in Pyrex vessels. These results are similar to those obtained by Elder and Rideal[12] for the reaction between hydrogen peroxide gas and liquid mercury.

It was still necessary to investigate the possibility of catalytic decomposition of hydrogen peroxide when high percentage liquid peroxide

TABLE I. Effect of warming the trap on hydrogen peroxide yield.

Expt. No.	Trap condition when rinsed	Product wt., mg	H_2O_2 wt., mg	H_2O_2 percent
74	Room temp.	100	79.7	79.7
75	Cold		81.6	
76	Room temp.	98	80.3	82.0
77	Cold		79.9	

[12] J. W. Elder, Jr. and E. F. Rideal, Trans. Faraday Soc. **23**, 545 (1927).

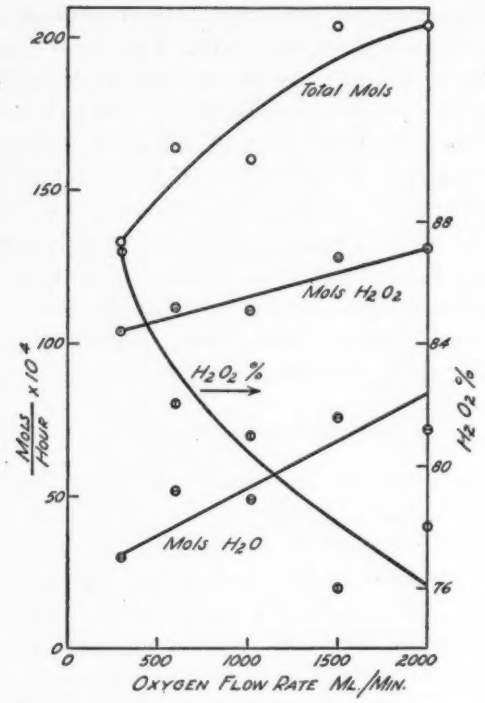

FIG. 2. Yield of product *versus* oxygen flow rate. Hydrogen flow fixed at 3000 ml/min.

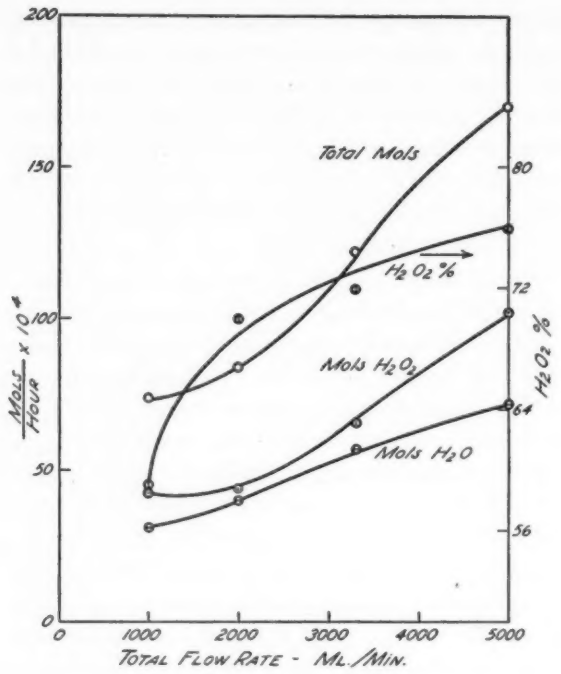

FIG. 3. Yield of product *versus* total flow rate. Hydrogen to oxygen ratio fixed at 3 to 2.

is in contact with liquid mercury. This could account for appreciable peroxide loss on warming the trap prior to weighing the final product. If the reaction results only in a stoichiometric loss of hydrogen peroxide caused by the reaction with the small quantity of mercury present, the amount decomposed should be negligible. Any decomposition loss should be avoided by rinsing out the trap immediately after removing from the liquid air and titrating the hydrogen peroxide. Since the trap cannot be weighed, it is not possible to determine the percent of peroxide in the reaction products when analysis is made in this manner. It may be seen from Table I that there is no observable loss caused by the interaction between mercury and hydrogen peroxide in the trap.

TABLE II. Variation of O_2 flow rate at constant H_2 flow of 3000 ml/min.

Expt. No.	O_2 flow ml/min	Product mg	H_2O_2 %	H_2O_2 moles/hr	H_2O moles/hr	Moles/hr total	ΦH_2O_2	Φ_T
115	300	68	94.8	0.0114	0.0012	0.0126	0.27	0.29
118	300	60	91.2	.0097	.0017	.0114	.23	.27
121	300	64	85.6	.0097	.0030	.0127	.23	.30
125	300	73	82.0	.0106	.0043	.0149	.25	.35
130	300	72	79.7	.0101	.0050	.0151	.23	.35
123	600	96	84.0	.0143	.0050	.0193	.33	.45
126	600	82	80.8	.0117	.0053	.0170	.27	.40
134	600	76	79.6	.0107	.0053	.0160	.25	.37
117	1000	75	81.5	.0118	.0047	.0165	.28	.39
120	1000	73	81.5	.0105	.0043	.0148	.25	.35
131	1000	80	79.0	.0111	.0057	.0167	.26	.39
122	1500	101	81.5	.0146	.0063	.0209	.34	.49
127	1500	88	76.7	.0119	.0067	.0186	.28	.43
129	1500	91	63.7	.0102	.011	.0213	.24	.50
132	1500	97	70.5	.0120	.0097	.0217	.28	.51
116	2000	91	81.5	.0131	.0057	.0188	.31	.44
119	2000	93	82.8	.0136	.0053	.0189	.32	.44
124	2000	96	76.2	.0129	.0077	.0206	.30	.48
128	2000	104	70.0	.0129	.010	.0229	.30	.54

The Quantum Yield

A determination of the incident quanta was made using uranyl oxalate as an actinometer.[13] The reaction vessel was filled with a solution

TABLE III. Variation of total flow rate at fixed H_2:O_2 ratio. Ratio of H_2:O_2 = 3:2.

Expt. No.	Total flow ml/min	Product mg	H_2O_2 %	H_2O_2 moles/hr	H_2O moles/hr	Moles/hr total
139	1000	31	56.5	0.00308	0.0043	0.00738
138	2000	39	65.5	.00450	.0043	.00880
148	2000	36	68.3	.00433	.0037	.00803
136	3300	54	70.9	.00675	.0053	.01205
149	3300	55	67.8	.00657	.0060	.01257
143	5000	68	73.8	.00893	.0060	.01493
146	5000	87	80.3	.0123	.0057	.0180
150	500	83	64.7	.00945	.0097	.01915

[13] W. G. Leighton and G. S. Forbes, J. Am. Chem. Soc. **52**, 3139 (1930).

containing 0.01 mole per liter uranyl oxalate and 0.05 mole per liter oxalic acid. After a known period of irradiation, an aliquot of the solution was titrated with standard 0.1 N potassium permanganate. The intensity of light entering the reaction cell was found to be 7.1×10^{-4} Einstein per minute. The quantum yields subsequently given are based on this value.

The Hydrogen-Oxygen Reaction

For experiments in which the flow rate of hydrogen was kept constant and the oxygen flow rate was varied, results are shown in Table II and Fig. 2.

The yield of product at varying total flow rate for a constant ratio of H_2O_2 was followed. The period of irradiation again was 10 minutes. Results are shown in Table III and Fig. 3.

Table IV and Fig. 4 show results obtained for a variation of H_2:O_2 ratio at a constant total flow rate of 3300 ml/min. The exposure time for these runs was also 10.0 minutes.

Reaction Between Ozone and Hydrogen Peroxide

Ozone may be formed by the photo-sensitized reaction of oxygen with mercury.[14] The reaction between ozone and hydrogen peroxide has been studied in aqueous solution by several investigators. The most extensive study was made by Taube and Bray,[15] and the following mechanism was advanced:

$$H_2O_2+O_3\rightarrow HO+HO_2+O_2, \quad (7)$$

$$HO_2+O_3\rightarrow HO+2O_2, \quad (8)$$

$$HO+O_3\rightarrow HO_2+O_2, \quad (9)$$

$$HO+H_2O_2\rightarrow HO_2+H_2O. \quad (10)$$

TABLE IV.

Expt. No.	H_2O_2 ratio	Product mg	H_2O_2 %	H_2O_2 moles/hr	H_2O moles/hr	Moles/hr total
142	10	46	74.0	0.00600	0.0043	0.00103
137	3	55	73.3	.00713	.0050	.01213
136	1.5	54	70.9	.00675	.0053	.01205
149	1.5	55	67.8	.00657	.0060	.01257
140	0.67	52	57.8	.00532	.0073	.01262
141	0.33	40	25.9	.00184	.0100	.0118

[14] R. G. Dickinson and M. S. Sherill, Proc. Nat. Acad. Sci. 12, 175 (1926).

[15] H. Taube and W. C. Bray, J. Am. Chem. Soc. 62, 3357 (1940).

Reaction (7) is the chain initiating step. (8) and (9) result in chain decomposition of ozone. (8) and (10) constitute a chain for the reaction between ozone and peroxide.

Since it was likely that ozone was being formed in our experiments, we were interested in determining whether the reaction occurred in the vapor phase and whether it could occur between a condensed phase of peroxide and ozone gas at low temperatures. Ozone was prepared by passing a measured amount of oxygen gas through a quartz tube under irradiation of a strong mercury discharge. Hydrogen peroxide was prepared by the mercury sensitized hydrogen-oxygen reaction. The streams containing ozone and peroxide were brought together in a mixing chamber, and the resulting product was condensed in a dry ice-alcohol trap. The results are given in Table V. Experiment *M*-1 shows the rate of ozone formation in the apparatus, and experiments *M*-3 and *M*-5 show the rate of product yield when no ozone is added. *M*-4 and *M*-6 show the effect of adding ozone. *M*-7 shows the effect of passing ozone over hydrogen peroxide previously trapped out.

It may be seen that ozone and H_2O_2 are present at the time of mixing in almost equal molal quantities. The reaction between ozone and H_2O_2 results in almost complete removal of H_2O_2 when the two are brought together in the gas phase. Passing ozone over H_2O_2 at dry ice temperature has no appreciable effect.

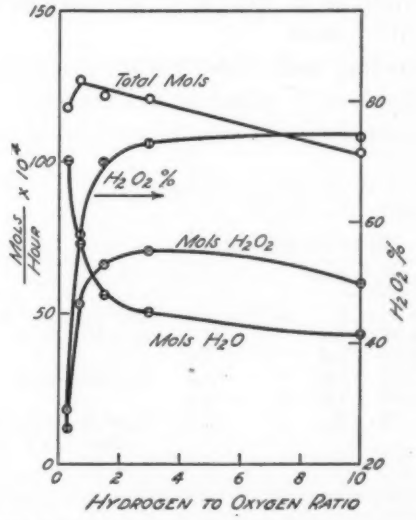

FIG. 4. Yield of product *versus* hydrogen to oxygen ratio. Total flow fixed at 3300 ml/min.

A very interesting observation is the fact that there seems to be a loss of hydrogen in the reaction products when hydrogen peroxide and ozone are mixed in the gas phase. A comparison of *M*-3, 5, 7 with *M*-4, 6 shows this to be the case. A discrepancy between the total moles of peroxide plus water for the experiments with and without adding ozone seems greater than can be accounted for by experimental error. This implies that the reactions involving the free radicals formed in the ozone-peroxide reactions produce gaseous hydrogen.

MECHANISM OF THE MERCURY SENSITIZED HYDROGEN-OXYGEN REACTION

The reaction scheme proposed by Bates[9] leads to the kinetic equation,

$$\frac{d(H_2O_2)}{dt}=\frac{k_4(H_2)}{k_5^{\frac{1}{2}}}\left(\frac{k_1 I_a(H_2)}{k_1(H_2)+k_2(O_2)}\right)^{\frac{1}{2}}+\frac{k_1 I_a(H_2)}{k_1(H_2)+k_2(O_2)}. \quad (a)$$

This mechanism purports to explain the rate variation with the concentration of hydrogen and oxygen and the variation of quantum yield with intensity of light. Objections to this correlation have already been formulated in the introduction to this paper. The quantum yields reported herein are also well below unity which, although not proof of a non-chain mechanism, allows the formulation of a non-chain mechanism at the temperature used.

Bonhoeffer and Haber[16] and Frankenburger and Klinkhardt[8] arrive at a mechanism which substitutes, for reactions (5) and (6) above, the reactions

$$HO_2+H_2\rightarrow H_2O+OH, \quad (11)$$

$$OH+OH\rightarrow H_2O_2, \quad (12)$$

and to explain quantum yields slightly above unity,

$$HO_2+H_2O\rightarrow H_2O_2+OH. \quad (13)$$

Much of the scheme is derived from the high yields of water found in their experiments. Bates and Salley[7] have shown that this formulation requires at least 51.4 percent water in the products. The high percentage yields of peroxide found in this and the earlier investigations are a refutation of this mechanism.

Surface effects, the complexity of exact kinetics in a flowing system, and the obscureness of the role played by activation entering the oxygen molecule make it difficult to establish the mechanism of the reaction. However, it is possible, on the basis of some reasonable assumptions, to arrive at a rate equation which seems to have some validity.

The results of Tables II and III indicate that the total moles of product depend upon both the flow rate and the composition of the gases. The fact that the total number of moles of product for a fixed hydrogen to oxygen ratio depends on the flow rate shows that hydrogen is being reformed by interaction between free radicals or H atoms.

Since it is possible to achieve yields of hydrogen peroxide upwards of 90 percent, we may assume that all water found is formed from hydrogen peroxide. This water may come from peroxide decomposing by an over-all equation,

$$2H_2O_2\rightarrow 2H_2O+O_2, \quad (14)$$

or water may come from the reaction between hydrogen peroxide and ozone, to which reference has already been made. If we assume that these water forming reactions are independent ones, then we can use the number of moles of product, water plus peroxide, as the number of moles of hydrogen peroxide formed in the reaction.

The adsorption of H atoms on quartz or Pyrex is strong, and it may be concluded that H atoms reaching the wall remain and eventually recombine to give hydrogen. We may then substitute for Eq. (5) the reactions,

$$H+M\rightarrow HM, \quad k_4' \quad (15)$$

TABLE V. The ozone-hydrogen peroxide reaction.

Expt. No.	Moles per hour ×10⁴				Remarks
	H_2O_2	H_2O	O_3	Total	
M-1	0	0	1.59	1.6	Only ozonizer operating
M-3	1.64	2.4	—	4.0	Ozonizer dark
M-4	0.19	2.8	—	3.0	
M-5	1.44	2.0	—	3.4	Ozonizer dark
M-6	0.13	3.0	—	3.1	
M-7	1.39	2.1	—	3.5	Ozonizer operating only after H_2O_2 synthesis stopped.

[16] K. F. Bonhoeffer and F. Haber, Zeits. f. physik. Chemie **137A**, 363 (1928).

the adsorption of H atoms on the walls, and

$$HM+HM\rightarrow H_2+M, \qquad (16)$$

the adsorption of H atoms on the walls, and

$$HM+HM\rightarrow H_2+M, \qquad (16)$$

the formation of hydrogen on the walls. This formulation eliminates the chain character of the mechanism of Bates and, using the steady-state method, leads to the kinetic equation,

$$\frac{d(H_2O_2)}{dt}=\frac{k_3(O_2)}{k_3(O_2)+k_4'M}\,\frac{I_ak_1(H_2)}{k_1(H_2)+k_2(O_2)}. \qquad (b)$$

Since the number of collisions of H atoms with the walls will be governed by the flow rate, the effective wall may then be considered as inversely proportional to the flow rate. For k_4' M, the expression k_4'' $1/F$, where F is the total flow rate, may be substituted. Expressed in terms of flow rates, the concentration of each species becomes the flow rate at which it is introduced into the system divided by the total flow rate. In terms of flow rates, the kinetic equation becomes,

$$\frac{d(H_2O_2)}{dt}=\frac{k_3/k_4''(O_2)}{k_3k_4''(O_2)+1}\,\frac{I_ak_1/k_2(H_2)}{k_1/k_2(H_2)+(O_2)}. \qquad (c)$$

k_1 and k_2 are the bimolecular rate constants for the quenching of activated mercury by hydrogen and oxygen. Zemansky[17] has shown that the relative quenching efficiencies of hydrogen and oxygen are 1.1 and 0.68, respectively. k_1k_2 in the rate expression then is equal to 1.1/0.68 or 1.62. I_a has been shown to be equal to 0.043 Einstein per hour.

It is hardly to be expected that experimental data would be closely fitted by the above expression, since variability of walls would be such an important factor. However, for data obtained over a small time interval and with consistent technique, some success might be expected. Using a ratio of $k_3/k_4''=1.2\times10^{-3}$, the rates for the condition represented in Table II have been calculated. Figure 5 shows a comparison of calculated rates, the curve, and the experimental values, circles. The k_3/k_4'' ratio indicates that reaction (15) occurs much more readily than reaction (3). This is a reasonable result since it would be expected that some means of dissipation of excess energy is necessary to stabilize HO_2 formed from H and O_2, while adsorption of H atoms on the wall should occur on almost every collision.

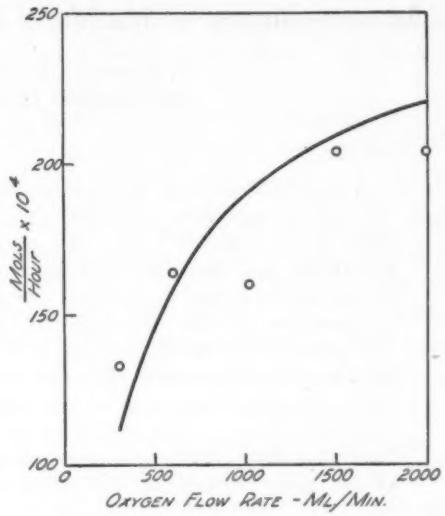

FIG. 5. Comparison of experimental values, circles, with calculated values, curve. Variation of oxygen flow rate for a fixed hydrogen flow of 3000 ml/min.

ACKNOWLEDGMENT

The assistance of Dr. Boris Leaf with some of the experimental work is gratefully acknowledged. The author also wishes to thank Professor W. H. Rodebush, Official Investigator in charge of the program, for his interest and the many valuable discussions.

[17] M. W. Zemansky, Phys. Rev. **36**, 919 (1930).

THE JOURNAL OF CHEMICAL PHYSICS VOLUME 14, NUMBER 12 DECEMBER, 1946

Investigation of Oxidation of Copper by Use of Radioactive Cu Tracer

J. BARDEEN, W. H. BRATTAIN, AND W. SHOCKLEY
Bell Telephone Laboratories, Murray Hill, New Jersey

(Received October 7, 1946)

A very thin layer of radioactive copper was electrolytically deposited on a copper blank. The surface was then oxidized in air at 1000°C for 18 minutes, giving an oxide layer with a thickness of 1.25×10^{-2} cm. After quenching, successive layers of the oxide were removed chemically, and the copper activity in each layer was measured. The observed self-diffusion of radioactive copper in the oxide agrees quantitatively with a theory based on the following assumptions: (a) The oxide grows by diffusion of vacant Cu^+ sites from the outer surface of the oxide inward to the metal. (b) The concentration of vacant sites at the oxygen-oxide interface is independent of the oxide thickness, and drops linearly from this constant value to zero at the metal boundary. (c) Accompanying the inward flow of vacant sites, there is a flow of positive electron holes such as to maintain electrical neutrality. (d) Self-diffusion of copper ions takes place only by motion into vacant sites. The results give a fairly direct confirmation of the theory of oxidation first suggested by Wagner.

I. INTRODUCTION

FRENKEL, Schottky, Jost, and particularly Wagner,[1] have explained ionic conductivity and diffusion in solids as resulting from certain types of lattice defects (departures from perfect periodicity) which are in equilibrium with the lattice at high temperatures. Wagner[2] has extended these ideas to explain rates of reactions in the solid state which are limited by the diffusion of one of the constituents.

At high temperatures, copper oxidizes in the presence of oxygen gas in the form of a uniform film of Cu_2O which, except for very thin films, increases in thickness proportionally with the square root of the time. The rate of growth increases rapidly with increasing temperature, and also depends on the oxygen gas pressure.[3] On the basis of a large number of experiments,[4] Wagner and co-workers have developed a theory to account for the reaction rate which includes the following assumptions:

(a) The lattice defects in Cu_2O are vacant sites ordinarily occupied by Cu^+ ions (so-called Schottky defects). These vacant sites have an effective negative charge of one electron.

(b) Electrical neutrality is maintained by an equivalent number of positive electron holes (electrons missing from the uppermost filled band). These electron holes are responsible for the electrical conductivity of Cu_2O.

(c) The electron holes and vacant sites are completely dissociated at temperatures of the order of 1000°C. There may, however, be incomplete disorder of the Debye-Hückel type.

(d) The equilibrium number of vacant sites depends on the pressure of the oxygen gas in contact with the oxide. The concentration in equilibrium with metallic copper is small. During oxidation, there is a concentration gradient of vacant Cu^+ sites extending from the oxygen interface to the metal.

(e) The oxide is formed at the oxygen interface. The Cu^+ ions arrive by diffusion from the metal through the oxide.

(f) The mechanism of diffusion of the Cu^+ ions is by motion of vacant sites from the oxygen interface to the metal.

(g) Electrical neutrality is maintained by an equal current of positive electron holes from the oxygen interface to the metal.

The equation for the reaction at the oxygen interface may be expressed in the form

$$O_2 \rightarrow 2\,Cu_2O + 4[Cu^+]_A + 4[e-]_A,$$

in which $[\ ]_A$ indicates a vacancy or defect Cu^+ ion or electron. Correspondingly, at the metal

[1] See, for example, W. Jost, *Diffusion und Chemische Reaktion in festen Stoffen* (T. Steinkopff, Dresden, 1937), or N. F. Mott and R. W. Gurney, *Electronic Processes in Ionic Crystals* (Oxford University Press, Oxford, 1940), Chaps. II and VIII.

[2] C. Wagner, Zeits. f. physik. Chemie **B21**, 25 (1933); **B32**, 447 (1936); C. Wagner and K. Grünewald, Zeits. f. physik. Chemie **B40**, 455 (1938). See also C. Wagner, Trans. Faraday Soc. **34**, 851 (1938), N. F. Mott, Trans. Faraday Soc. **36**, 472 (1940).

[3] N. B. Pilling and R. E. Bedworth, J. Inst. Metals **29**, 529 (1923). A logarithmic law is followed at low temperatures. Cf. B. Lustman and R. F. Mehl, Metals Tech. **8**, 1317 (1941).

[4] The first comprehensive experiments are those of H. Dünwald and C. Wagner, Zeits. f. physik. Chemie **B22**, 212 (1933). Later experiments, together with a comparison of theoretical and experimental values for the rate of oxidation, are summarized by C. Wagner and K. Grünewald, reference 2.

interface

$$Cu+[Cu^+]_h+[e-]_h \rightarrow \text{normal lattice.}$$

The vacant Cu^+ sites are filled by Cu^+ ions from the metal and the electron defects are filled by electrons from the metal thus eliminating the two holes and leaving the normal lattice in their place. Except when the oxide layer is very thin, the rate of reaction is limited by diffusion of the vacant sites from the oxygen interface to the metal. A very much simplified version of Wagner's theory is given in Section III.

It may be appropriate to make some brief remarks about the experimental basis for Wagner's assumptions. Wagner and co-workers[4] have measured the rate of oxidation, and also a number of properties of Cu_2O in equilibrium with O_2, at various pressures, with the following conclusions:

(a) The rate constant for oxidation varies with oxygen pressure as $p^{1/7}$.

(b) The electrical conductivity[5] is also proportional to $p^{1/7}$.

(c) The stoichiometric excess of O in Cu_2O, as determined chemically,[6] is proportional to $p^{1/5}$.

(d) The transport number[7] for ionic conduction in Cu_2O indicates that vacant Cu^+ sites carry 5×10^{-4} of the current at 1000°C.

Elementary theory, assuming complete dissociation of electron defects, and vacant sites, predicts that the excess oxygen should vary as $p^{1/8}$. Complete association would give a $p^{1/4}$ dependence. The observed $p^{1/5}$ dependence is intermediate, suggesting partial dissociation. Another possibility, suggested by Wagner and Hammer,[6] is that dissociation is complete, but that there is incomplete disorder of the Debye-Hückel type. If it is assumed that dissociation is complete, so that there are two defect electrons for each excess O atom, the number of electrons as determined from the stoichiometric excess, together with the electrical conductivity, indicate a mobility of about 1 cm²/volt sec. at 1000°C.[8] This value is only a little smaller than one would predict from extrapolations of mobilities determined from the Hall effect at lower temperatures. Thus a reasonable fraction of the centers must be dissociated.

As outlined in Section III, Wagner has shown that the rate of reaction can be determined from the equilibrium number of vacant sites, the electrical conductivity, and the transport number. Assuming complete dissociation, approximate agreement with directly measured values was obtained.[4] This agreement, together with the fact that the rate constant varies with pressure in the same way as the electrical conductivity, indicates that diffusion during oxidation is mainly by dissociated vacant sites. If there is an appreciable number of neutral associated centers, their mobility must be so small that they do not contribute appreciably to the reaction.

In order to investigate further the diffusion of copper ions during oxidation, we have performed an experiment using a radioactive copper tracer. A thin coating of radioactive copper was electroplated on a copper blank. The surface was oxidized in air at atmospheric pressure at a temperature of 1000°C for 18 minutes, giving an oxide film with a thickness of about 0.0127 cm. The distribution of radioactive copper in the film was then determined. We are here concerned with the self-diffusion of copper in Cu_2O which has a varying concentration of vacant sites.

There are two possible mechanisms for self-diffusion:

(a) Motion of copper ions into vacant sites. This mechanism will contribute a term to the diffusion coefficient proportional to the concentration of vacant sites.

(b) Interchange of two neighboring Cu^+ ions in the lattice. The probability should be independent of the concentration of vacant sites.

Our results indicate that the mechanism of self-diffusion is (a) rather than (b). Good agreement between calculated and experimental results is obtained if the distribution of vacant sites is assumed to vary in position and time in accordance with Wagner's theory of the oxidation reaction. Our results thus confirm Wagner's theory, without reference to conductivity experiments.

II. EXPERIMENTAL PROCEDURE AND RESULTS

The experimental work described in this paper was done in 1938, but publication was delayed

[5] J. Gundermann, K. Hauffe, and C. Wagner, Zeits. f. physik Chem. **B37**, 148 (1937).

[6] C. Wagner and H. Hammer, Zeits. f. physik Chemie **B40**, 197 (1938).

[7] J. Gundermann and C. Wagner, Zeits. f. physik Chemie **B37**, 155 (1937).

[8] There is apparently a numerical error of a factor of ten in the calculations of reference 6.

TABLE I. Determination of the thicknesses of oxide layers from change in weight during etching.

Sample	Weight in grams before	after	diff.	Thickness in cm
1	8.097	7.936	.161	1.6×10^{-3}
2	7.936	7.469	.467	4.67×10^{-3}
3	7.469	7.121	.348	3.48×10^{-3}
4*	7.121	6.714	.407	
Oxide in 4**			.300	3.00×10^{-3}
Total oxide			1.27	12.7×10^{-3}

* This includes some of the underlying copper.
** By difference.

TABLE II. Percent of radioactive copper in successive layers as determined from tests of activity.

Sample	Wt. of Cu tested mg	Counts in 5 min.	Counts per min. per mg corrected for background	Percent of total activity in sample
1	21	218	1.2	22.5±2
2	17	180	1.0	55.0±6
3	27	155	0.45	17.5±2.5
4	27	108	0.11	5.0±2.5

because the results are rather incomplete. Because of the stress of other work and the intervention of the war, further experimental work has been postponed indefinitely so that it has been decided to publish the available data, together with a recent theoretical analysis of the problem, at this time.[9]

The copper blank used in the experiment was electroplated with radioactive copper by J. Steigman, then at Columbia University. The technique used is exactly the same as that used for the preparation of blanks for a study of the self-diffusion of copper in the metal, done about the same time.[10]

Sufficient radioactive copper (Cu 64, period of decay, 12.8 hours) was deposited on one side of a copper blank, to give an activity of about 2000 counts per minute. The blank was then oxidized in air at atmospheric pressure at 1000°C for 18 minutes, was kept at 500°C for 3 minutes, and then quenched in air. The oxide film was formed only on the active side of the blank. The back of the blank was protected by another sheet of copper. At 1000°C the oxide film formed is all Cu_2O. At 500°C a thin film of black CuO is formed on the surface of the Cu_2O. The total thickness of the oxide was determined by the increase in weight of the copper blank after oxidation (weight of O_2 absorbed). This thickness was 12.7×10^{-3} cm. The CuO layer was less than 10 percent of this.

Successive layers of oxide were removed by etching the oxidized face of the copper blank in nitric acid. After each etch the blank was washed in water, dried, and weighed. These weights and the calculated thickness of oxide in each sample are given in Table I. The nitric acid and the water used in washing the blank after each etch were saved. The copper from each successive etch was precipitated from the mixture of nitric acid and wash water as copper sulfide. Four successive layers were etched off. The last one included some of the underlying copper.

Some of the wet copper sulfide powder from each sample was tested for activity by spreading it out on filter paper, allowing it to dry, and wrapping it around the counter. The results of these tests are given in Table II. The total activity in each layer is determined by multiplying the activity per mg by the total weight of each sample (see Table I). The last column gives this activity in percent. The probable errors listed were determined from the number of counts. Other possible errors are smaller.

III. WAGNER'S THEORY OF OXIDATION

Wagner's theory of oxidation, as applied to the formation of Cu_2O, may be outlined briefly as follows.[11] Let x represent the distance of a point in the oxide from the metal surface. Let $n_e(x)$ and $n_i(x)$ represent the concentrations (number per cm^3) of (dissociated) defect electrons and vacant sites, respectively. For an electrostatic field $F(x)$ in the oxide, the electronic and ionic current densities, from both diffusion and conduction, are

$$I_e = -eD_e(\partial n_e/\partial x) + \sigma_e F(x) \quad (1)$$

and

$$I_i = eD_i(\partial n_i/\partial x) + \sigma_i F(x), \quad (2)$$

[9] The experimental work was done by the second and third named authors. The first named author has been concerned only with the theoretical interpretation and analysis of results.

[10] The method is described by J. Steigmann, W. Shockley, and F. C. Nix, Phys. Rev. **56**, 13 (1939). See also J. Steigmann, Phys. Rev. **53**, 771 (1938).

[11] The following is a much simplified version of Wagner's theory, and is presented to introduce equations needed for later reference. Cf. N. F. Mott, reference 2.

where D and σ represent diffusion coefficients and conductivities, respectively. For equal concentrations, D_e and σ_e differ from D_i and σ_i by the ratio of the electronic to the ionic mobilities, a large factor.[12]

Since the space charge is limited, $n_e \simeq n_i$ throughout most of the layer. Each term on the right of Eq. (1) therefore differs from the corresponding term of Eq. (2) by the ratio of the mobilities. Furthermore, since there is no net current, $I_e = -I_i$, so that I_e must be small compared with either term on the right-hand side of Eq. (1). In other words, I_e represents a small difference between two nearly equal terms. The electrostatic field, $F(x)$, of course, adjusts in such a way that these conditions are satisfied. Since the two terms on the right-hand side of Eq. (2) differ from those of Eq. (1) by a constant factor, they must also be nearly equal. However, instead of subtracting, they add, so that we have approximately

$$I_i = 2eD_i(\partial n_i/\partial x). \tag{3}$$

Consequently the effect of the electrostatic field in the oxide is to double the current to be expected from diffusion alone. Equation (3) is a special case of a more general expression derived by Wagner, which was in turn based on a similar equation for the diffusion of electrolytes.

Except during the initial stages, the rate of oxidation is controlled by diffusion of Cu from the metal to the oxygen interface. Diffusion of a vacant Cu^+ site from the oxygen interface to the metal is equivalent to the motion of one Cu^+ ion from the metal to the outside surface. The copper ion current (ions per unit area per unit time) can be obtained from the current (3) by dividing by e, the charge per ion. This current must be divergenceless (except for a very small contribution used to readjust the value of n_i as the layer grows). Consequently, $\partial n_i/\partial x$ is independent of x through the layer.

Let $X(t)$ be the thickness of the oxide layer at time t, and suppose that in time dt the thickness increases by dX. Let N be the normal number of Cu^+ ions per unit volume. The number of Cu^+ ions which diffuse in time dt is then equal to NdX, and making use of Eq. (3),

$$\frac{dX}{dt} = \frac{2D_i}{N}\frac{\partial n_i}{\partial x}. \tag{4}$$

It is assumed that the concentrations of vacant sites at the metal and oxygen interfaces are determined by local reactions and are independent of the thickness of the layer. Denoting their difference by Δn_i we have

$$\partial n_i/\partial x = \Delta n_i/X. \tag{5}$$

If Eq. (5) be substituted into Eq. (4), we find that the rate of growth is inversely proportional to the oxide thickness,

$$dX/dt = K/X, \tag{6}$$

where the rate constant K is

$$K = 2D_i\Delta n_i/N. \tag{7}$$

The thickness at time t as obtained from integration of (6) is

$$X = (2Kt)^{\frac{1}{2}} = 2(D_i t\Delta n_i/N)^{\frac{1}{2}}. \tag{8}$$

The approximate validity of Eqs. (7) and (8) has been checked by Wagner and Grünewald.[2] The coefficient of diffusion was obtained from Einstein's relation, $eD_i = v_i kT$. The mobility v_i was derived from measurements of the transport number for ionic conduction, τ_i, the electrical conductivity, σ, and the number of vacant sites, n_i (the latter from the stoichiometric excess of 0):

$$v_i = \sigma\tau_i/en_i.$$

Thus, in terms of measured quantities,

$$K = (2\sigma\tau_i kT/e^2N)(\Delta n_i/n_i). \tag{7a}$$

This expression, which is slightly different from the one used by Wagner and Grünewald, gives good agreement with the observed rate of reaction. It should be noted that only the relative values of the concentration of vacant sites appears. An appreciable number of associated centers (defect electrons+vacant sites) could exist without affecting the agreement provided that

(a) The degree of dissociation does not vary greatly with concentration.

(b) The diffusion constant of associated centers is considerably less than that of dissociated vacant sites.

[12] About 2×10^3 at 1000°C (reference 6).

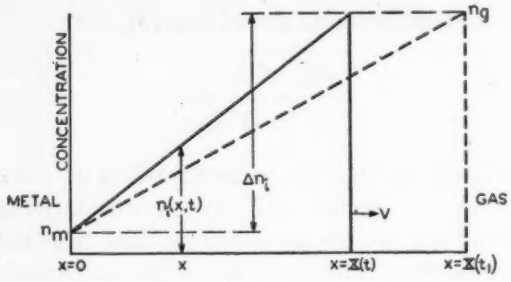

FIG. 1. Schematic diagram of oxide layer showing concentration $N_i(x, t)$ of vacant Cu^+ sites at successive times.

IV. THEORY OF DIFFUSION OF RADIOACTIVE Cu

One mechanism by which diffusion of radioactive Cu can take place is by motion into a vacant lattice site. The vacant site may move into any neighboring site, but a Cu^+ ion will diffuse only if a neighboring Cu^+ site is vacant. This mechanism will give a contribution to the self-diffusion coefficient for Cu^+ ions equal to the diffusion coefficient for vacant sites, D_i, times the probability that a given neighboring site is vacant, n_i/N. This part of the self-diffusion coefficient may depend both on the position within the oxide layer and on the time:

$$D_i n_i(x, t)/N. \tag{9}$$

According to Eq. (5), the concentration of vacant sites varies linearly with x, increasing from a small value, n_m, at the metal interface to $n_g = n_m + \Delta n_i$ at the oxygen interface. We may set

$$n_i(x, t) = n_m + x\Delta n_i/X. \tag{10}$$

We assume n_m and Δn_i are constant, and that the thickness of the layer, X, increases with time according to Eq. (8).

In addition to diffusion by motion into vacant sites, it is conceivable that two adjacent Cu^+ ions may change places. This would give a constant contribution to the self-diffusion coefficient, indistinguishable from that resulting from a uniform distribution of vacant sites, as obtained, for example, from the constant term n_m in Eq. (10). Thus we assume for the self-diffusion coefficient, D, for Cu^+ ions:

$$D = D_0 + D_i \frac{\Delta n_i}{N} \frac{x}{X}. \tag{11}$$

Replacing X by its value from Eq. (8),

$$D = D_0 + \tfrac{1}{2}(D_i \Delta n_i/N)^{\frac{1}{2}}(x/t^{\frac{1}{2}}). \tag{12}$$

We are now ready to derive the self-diffusion equation appropriate during oxidation. Figure 1 shows the oxide layer at any time t. The concentration of vacant sites increases linearly from n_m at the metal interface ($x=0$) to n_g at the oxygen interface ($x=X$). The oxygen interface is moving to the right with a velocity

$$V = dX/dt = (D_i \Delta n_i/Nt)^{\frac{1}{2}}. \tag{13}$$

The current of radioactive Cu^+ ions at any point x in the layer will be the sum of two terms: a diffusion current, $-D(\partial c/\partial x)$, due to the concentration gradient, and a drift term, Vc, proportional to the concentration, which comes from the drift of Cu^+ ions from the metal to the oxygen interface as the layer grows. Thus the total current is

$$-D(\partial c/\partial x) + Vc. \tag{14}$$

The rate of change of concentration with time is equal to the negative of the gradient of the current

$$\frac{\partial c}{\partial t} = -\frac{\partial}{\partial x}\left(-D\frac{\partial c}{\partial x} + Vc\right) = D\frac{\partial^2 c}{\partial x^2} - \left(V - \frac{\partial D}{\partial x}\right)\frac{\partial c}{\partial x}. \tag{15}$$

Comparison of (12) and (13) shows that

$$V = 2(\partial D/\partial x), \tag{16}$$

so the diffusion equation becomes

$$\frac{\partial c}{\partial t} = D\frac{\partial^2 c}{\partial x^2} - \frac{\partial D}{\partial x}\frac{\partial c}{\partial x}, \tag{17}$$

with D given as a function of x and t by Eq. (11) or (12).

There is a quasi-stationary solution of Eq. (17) of the form

$$c = \frac{1}{t^{\frac{1}{2}}} g(x/X), \tag{18}$$

which keeps the same shape as the layer increases in thickness, with the concentration at similar points decreasing inversely with the square root of the time. Regardless of the initial conditions

existing when the layer is very thin, this solution will be approached as the layer increases in thickness. This is the solution of interest.

In order to simplify the resulting equations, we set

$$z=x/X, \tag{19}$$

$$D_1=D_i\Delta n/N, \quad \alpha=D_0/D_i, \tag{21}$$

so that we have the following:

$$D=D_0+D_1Z=D_1(\alpha+z), \tag{22}$$

$$\frac{\partial c}{\partial t}=-\frac{1}{2t^{\frac{1}{2}}}g-\frac{1}{2t^{\frac{1}{2}}}z\frac{dg}{dz}, \tag{23}$$

$$\frac{\partial D}{\partial x}\frac{\partial c}{\partial x}=\frac{1}{t^{\frac{1}{2}}}\frac{D_1}{X^2}\frac{dg}{dz}=\frac{1}{4t^{\frac{1}{2}}}\frac{dg}{dz}, \tag{24}$$

$$\frac{\partial^2 c}{\partial x^2}=\frac{1}{t^{\frac{1}{2}}}\cdot\frac{1}{X^2}\frac{d^2g}{dt^2}=\frac{1}{4D_1t^{\frac{1}{2}}}\frac{d^2g}{dz^2}. \tag{25}$$

Substituting into Eq. (17) yields an ordinary differential equation,

$$(z+a)\frac{d^2g}{dz^2}+(2z-1)\frac{dg}{dz}+2g=0. \tag{26}$$

This equation may be expressed in the form

$$\frac{d}{dz}\left((z+\alpha)\frac{dg}{dz}+2(z-1)g\right)=0. \tag{27}$$

The interpretation is that the gradient of the current in the relative coordinate system (z coordinates) is zero. This is the requirement for quasi-stationary solution.

Since the flow of radioactive Cu^+ ions is zero at the oxygen interface ($z=1$), the current itself must vanish:

$$(z+\alpha)\frac{dg}{dz}+2(z-1)g=0. \tag{28}$$

In terms of the x coordinate system, Eq. (28) implies that

$$-D(\partial c/\partial x)+Vc=0 \text{ at } x=0,$$
$$-D(\partial c/\partial x)=0 \text{ at } x=X.$$

There is no flow of radioactive Cu^+ ions from the oxide to the metal ($x=0$), and, of course, no flow at the oxide-oxygen interface.

Equation (28) may be integrated directly to give:

$$g=A(z+\alpha)^{2(1+\alpha)}e^{-2z}, \tag{29}$$

where A is a constant of integration, determined by the total amount of radioactive copper present in the oxide.

In our case, only a negligible fraction of radioactive copper will diffuse into the metal; practically all will remain in the oxide.[13] The concentration would, however, follow the same law (Eq. (29)) even if diffusion into the metal were appreciable. The constant A would then be determined by the fraction of the total amount of radioactive copper in the oxide, which would depend on the diffusion into the metal, as well as on the total amount initially present. Once the quasi-stationary solution is attained, the fractions in the oxide and metal will remain fixed, as there is no further flow from the oxide to the metal.

The final solution may be expressed explicitly as follows:

$$c(x,t)=\frac{A}{t^{\frac{1}{2}}}\left(\frac{x}{X}+\frac{D_0}{D_1}\right)^{2(D_1+D_0)/D_1}e^{-2x/X}, \tag{30}$$

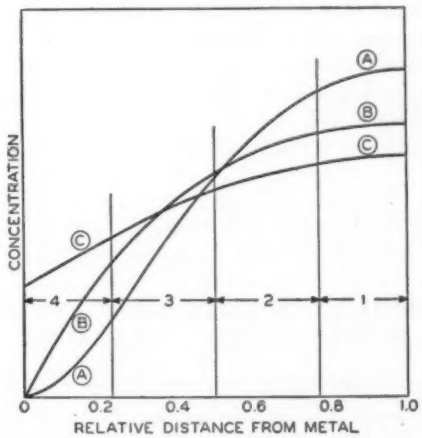

FIG. 2. Calculated concentrations of radioactive copper in oxide layer based on the following assumptions: Curve (A)—(1) self-diffusion takes place only by motion into vacant Cu^+ ion sites, (2) concentration of vacant sites increases linearly from 0 at the metal interface to a constant value at the oxygen interface ($\alpha=0$), (3) complete dissociation of centers composed of vacant Cu^+ sites and defect electrons; Curve (B)—same as (A) except that centers are *undissociated;* Curve (C)—same as (A) except that there is an additional mechanism of diffusion, giving a contribution to the diffusion coefficient independent of position in the oxide, and equal in magnitude to that caused by motion into vacant sites at the oxide-oxygen interface ($\alpha=1$).

[13] The self-diffusion coefficient of Cu in the metal is of the order 10^{-9} at 1000°C, as compared with a self-diffusion coefficient of the order 10^{-7}, for Cu in Cu_2O in equilibrium with air at atmospheric pressure and also at 1000°C.

TABLE III. Calculated and observed values of percent of total activity in successive layers of oxide. z=fractional distance from metal to oxygen interface. $D=D_1(\alpha+z)$ =self-diffusion coefficient for Cu^+ ions. Calculated values of activity are given for different values of α and for assumptions of both complete dissociation and no dissociation of centers composed of vacant Cu^+ ion sites and defect electrons.

Sample	Range of z	Observed	Calculated Dissociated $\alpha=0$	0.1	0.25	0.50	Undissoc. $\alpha=0$
1	0.77–1.00	22.5%	21%	20%	18%	17%	18%
2	0.50–0.77	55.	54	52%	50%	46%	48
3	0.22–0.50	17.5	21	22%	23%	25%	26
4	0–0.22	5.	4	6%	9%	12%	8

with D_0 and D_1 defined by Eqs. (11) and (20), and X, the thickness of the oxide layer given by (8). In terms of D_1,

$$X=2(D_1t)^{\frac{1}{2}}. \tag{31}$$

Figure 2 gives a plot of the calculated concentrations of radioactive Cu as a function of the relative distance from the metal for three different assumptions concerning the self-diffusion coefficient:

(A) Complete dissociation of vacant Cu ion sites and defect electrons, and $D_0=\alpha=0$.

(B) No dissociation of vacant Cu ions sites and defect electrons, and $D_0=\alpha=0$. This case is discussed briefly in the following section (see Eq. (33)).

(C) Complete dissociation, but with $D_0=D_1$, so that $\alpha=1$.

It is shown in the following section that (A) is in best agreement with experimental data.

V. COMPARISON OF THEORETICAL AND EXPERIMENTAL VALUES; CONCLUSIONS

Since the thickness of the samples removed by etching were not small compared with the total thickness of the oxide, comparison with theory is best made by using the fraction of the total activity in each sample. If the sample extends from $z=z_1$ to $z=z_2$, the fraction of the total activity to be expected can be obtained by integration of Eq. (27)

$$f=\frac{\int_{z_1}^{z_2}(z+\alpha)^{2(1+\alpha)}e^{-2z}dz}{\int_0^1(z+\alpha)^{2(1+\alpha)}e^{-2z}dz}. \tag{32}$$

For $\alpha=0$, the integration is elementary. For $\alpha\neq0$, the integrals can be expressed in terms of the incomplete Γ function, for which tables are available.

Table III gives the experimental values of f, expressed in percentages, as obtained from Table II, and the theoretical values obtained from Eq. (32), for $\alpha=0$, 0.1, 0.25, and 0.5. Complete dissociation of defect electrons and vacant sites is assumed. Good agreement (within the experimental uncertainties) is obtained for $\alpha=0$. The agreement is almost as good for $\alpha=0.1$, but is definitely worse for larger values of α. Thus we conclude that α is most probably not greater than about 0.1, and may be considerably smaller.

Results of Wagner and Grünewald[2] indicate that the fractional concentration of vacant Cu^+ sites in equilibrium with metallic copper is about 1.2×10^{-4} as compared with about 17×10^{-4} in equilibrium with air at atmospheric pressure, both at 1000°C. These values would give:

$$\alpha=\frac{1.2\times10^{-4}}{17\times10^{-4}}=0.07.$$

Our results are consistent with this value for α.

Self-diffusion by interchange of Cu^+ ions in neighboring positions must be small compared with diffusion *via* vacant sites, if it exists at all, under the conditions of our experiment.

Some information can also be obtained concerning the degree of association of defect electrons and vacant Cu^+ sites. Without more complete data and analysis it is difficult to set limits. If there were complete *association*, the centers would migrate by diffusion alone, so the factor of two would be missing from Eq. (3). The factor of 2 in Eq. (8) would be replaced by $\sqrt{2}$. The factor of 2 would also be missing from Eq. (16), and the second term on the right-hand side of Eq. (17) would not appear. The analysis can carried through for this case, leading to a distribution function for radioactive Cu of the form

$$g(z)=(z+\alpha)^{1+\alpha}e^{-z}. \tag{33}$$

The agreement with observed data is again best for $\alpha=0$, but is not nearly as good as that obtained for the assumption of complete dissociation. Values obtained from integration of Eq.

(33) with $\alpha=0$ are given in the last column of Table III. We conclude that either

(a) Dissociation is nearly complete or

(b) Dissociation is not complete, but the mobility of dissociated centers is much greater than that of undissociated centers.

As far as our results go, they are in complete accord with Wagner's. It is interesting to note that the numerical agreement between calculated and observed activities is obtained without introducing any empirical constants and without reference to any absolute values for diffusion coefficients or conductivities. The shape of the concentration curve is determined entirely by the mechanisms assumed for the oxidation reaction and for the self-diffusion of radioactive Cu^+.

THE JOURNAL OF CHEMICAL PHYSICS VOLUME 14, NUMBER 12 DECEMBER, 1946

A Proposed Interpretation of the Zeta-Potential

LAWRENCE B. ROBINSON
Department of Physics, Howard University, Washington, D. C.

(Received September 21, 1946)

The method used by Gurney and Fowler in explaining the interfacial potential at a metal-solution boundary is applied to the zeta-potential. This gives the ζ-potential as a straight line function of the logarithm of the concentration, in agreement with the shape of the curves as found experimentally. To obtain exact agreement between theory and experiment, it is proposed that the dielectric constant of the electrical double layer is about 0.6 that of the value for pure water. This assertion can be checked by accurate measurements on the surface conductance of solution of electrolytes.

INTRODUCTION

A SATISFACTORY theory correlating the zeta-potential with the concentration of the electrolyte in an aqueous solution has not been devised. Most of the recent attempts at constructing a theory[1] have been used on the idea of the Gouy double layer. The mathematical treatment utilizes solutions of the Poisson-Boltzmann equation

$$\nabla^2\psi=-\frac{4\pi\epsilon}{D}\sum_{i=1}^{s}n_iz_i\exp\left(-\frac{z_i\epsilon\psi}{kT}\right), \qquad (1)$$

with special boundary conditions. Insufficient and unreliable experimental information has been largely responsible for the failure of most of the attempts. Below, attention is called to a method which is believed to be more fruitful than previous approaches to the problem. Improvements and modifications of this method, in the light of additional experimental information, will probably yield an adequate theory. The method employed here has been used by Gurney[2] and Fowler[3] in explaining the metallic electrode potential, and by Dole[4] in explaining the glass electrode potential.

Recently significant gains have been made in regard to the experimental knowledge concerning the potential existing at the interface between vitreous silica and aqueous solutions of electrolytes. Hitherto there has been no agreement among the various experimenters[5] in this

[1] G. Gouy, J. Phys. [4], **9**, 457 (1910); D. L. Chapman, Phil. Mag. **25**, 475 (1913); O. Stern, Z. Electrochem. **30**, 508 (1924); A. March, Trans. Faraday Soc. **31**, 1468 (1935); A. J. Rutgers and Ed. Verlende, Proc. Kon. Akad. v. Wetensch. Amsterdam **42**, 71 (1939).

[2] R. W. Gurney, Proc. Roy. Soc. **A134**, 137 (1931); **A136**, 378 (1932); R. W. Gurney, *Ions in Solution* (Cambridge University Press, Cambridge, 1936), pp. 85–88.

[3] R. H. Fowler, Proc. Roy. Soc. **A136**, 391 (1932); Trans. Faraday Soc. **28**, 368 (1932).

[4] M. Dole, J. Chem. Phys. **2**, 862 (1934); M. Dole, *Experimental and Theoretical Electrochemistry* (McGraw-Hill Book Company, Inc., New York, 1935), pp. 512–515; M. Dole, *The Glass Electrode* (John Wiley and Sons, New York, 1941), pp. 261–276.

[5] H. Lach and J. Kronman, Bull. Int. de L'Acad. Polonaise d. Sci. d. Let. [A], Sci. Math. 289 (1925); H. Freundlich and G. Ettish, Zeits. f. physik. Chemie **116**, 401 (1925); H. R. Kruyt and van der Willigen, Kolloid Zeits. **45**, 307 (1928); Furutani, Kurokochi, and Asoda, Jap. J. Gastroent. **2**, 148 (1930); H. Lachs and J. Biczyk, Zeits. f. physik. Chemie **A148**, 441 (1930); R. duBois and

field, and the reliability of much of the data is open to question. Many experimenters have not characterized their methods and instruments adequately, and, therefore, a valid evaluation of their results is difficult. A hopeful indication that reliable information has been obtained concerning these potentials is furnished in the work of Rutgers and deSmet[6] at Ghent (Belgium) and Jones, Wood, and Robinson[7] at Harvard. This is perhaps the first time that systematic agreement has been obtained by different investigators, using different experimental techniques. Rutgers and deSmet, using the method of electro-endosmosis, studied the ζ-potential of solutions of metallic nitrates in contact with Jena 16 III glass, whereas the Harvard experimenters studied solutions of metallic chlorides in contact with quartz. The latter group used the streaming potential method. It is remarkable that the results were practically identical.

An interesting regularity was observed in both sets of data. Instead of the curves passing through maxima, as shown in most textbooks,[8] the potentials decreased in a more or less linear fashion with the logarithm of the concentration. Both groups of workers found out that thorium salts did not fit the general behavior pattern. Hydrolysis and other effects with thorium salts give their solutions properties not common to the other electrolytes. In developing a theory, one must look for a method of making the zeta-potential a straight-line function of the concentration.

METHOD OF GURNEY AND FOWLER

The assumptions used in this discussion are not entirely those used by Gurney, and the mathematical description is largely that employed by Fowler. Ions in solution are assumed to be affected by electrostatic and thermal forces, whereas the ions adsorbed at the surface are acted upon by specific adsorption forces in addition to the aforementioned types. This concept has been used before by A. March,[9] among others. Let U_m be the lowest energy level of anions adsorbed on the silica surface; it is assumed that the phase boundary is impervious to cations to the extent that no cations are adsorbed on the quartz surface. Let U_a be the lowest energy level of anions in the bulk of solution i.e., energy of the anions without thermal motion. The corresponding energy for cations is U_c but is uninteresting at the moment. The anions are able to make transitions from equilibrium positions in solution to equilibrium positions on the surface of vitreous silica. At the same time anions already deposited on the surface, having high enough energies, are able to make reverse transitions and resume equilibrium positions near water molecules. When kinetic equilibrium is established, the number of ions depositing on the surface is equal to the number leaving the surface dissolving in solution (per unit time). It is assumed that the Boltzmann distribution prevails both in solution and on the quartz surface.

The problem to be discussed is that of the equilibrium between anions in solution and on the vitreous silica surface. The anions in solution are not entirely free but are bound to water molecules or to groups of water molecules. The partition function for the anions in solution is

$$Q_{\text{solution}} = Ww(T) \sum_{i=0}^{\infty} p_i \exp\left[-U_i/kT\right], \quad (2)$$

where W represents the number of water molecules available for each anion and $w(T)$ represents the partition function for each water molecule. p_i is the statistical weight of each state of energy U_i; it is quite likely that the perturbation resulting from interacting levels makes each p_i equal to unity. In the absence of any interfacial potential ζ, the partition function for an anion on the vitreous silica surface would be

$$Q_{\text{silica}}(\zeta = 0) = \sum_{j=0}^{\infty} p_j \exp\left[-U_j/kT\right], \quad (3)$$

A. H. Roberts, J. Phys. Chem. **40**, 543 (1936); A. J. Rutgers, Ed. Verlende, and M. Moorkens, Proc. K. Ned. Akad. Wetensch. Amsterdam **41**, 763 (1938); A. J. Rutgers, Trans. Faraday Soc. **36**, 69 (1940).

[6] A. J. Rutgers and M. deSmet, Trans. Faraday Soc. **41**, 768 (1945).

[7] G. Jones and L. A. Wood, J. Chem. Phys. **13**, 106 (1945); L. A. Wood and L. B. Robinson, J. Chem. Phys. **14**, 251 (1946); L. B. Robinson, Ph.D. Thesis, Harvard University, Cambridge 38, Mass., May 1946, p. 125 and p. 162.

[8] H. A. Abramson, *Electrokinetic Phenomena* (Chemical Catalogue Co., 1934), p. 203; S. Glasstone, *Text-Book of Physical Chemistry* (D. Van Nostrand, 1940), p. 1201; S. Glasstone, *Introduction to Electrochemistry* (D. Van Nostrand, 1942), p. 534.

[9] A. March, Trans. Faraday Soc. **31**, 1468 (1935).

where the symbols have the same meaning as before. The existence of an interfacial potential ζ shifts each energy level by an amount $z\epsilon\zeta$ with respect to the condition given in (3). Consequently the correct partition function for the ions on the surface is

$$Q_{\text{silica}}=\sum_{j=0}^{\infty} p_j \exp\left[-(U_j+z\epsilon\zeta)/kT\right]. \quad (4)$$

The assumption is also made that the specific adsorption forces holding the ions on the surface are of the same nature as those which hold the units of the vitreous state. Evidence shows that the forces existing between particles in the vitreous state are similar to those which exist in the crystalline state. Hence the adsorbed ions may be treated as units of a crystal; the problem is now the same as that of a metallic crystal and its ions in solution. The additional assumption is made that the number of adsorbed anions, on the surface of the silica, is a constant independent of the concentration of the solution (in the limited concentration range in question), i.e. the adsorbed ions are fixed to a finite number of adsorbing centers. Gurney, Fowler, and Dole with their models, assumed that the probability of a transition from the surface to the solution depended only on the number of water molecules in the vicinity of the surface. Here the additional assumption is used that the number of transitions in a given time depends also on the number of adsorbed ions. This, however, is a constant and contributes nothing to the form of the partition function.

Fowler[10] shows that the equilibrium condition in terms of the partition functions is

$$n=W\frac{Q_{\text{solution}}}{Q_{\text{silica}}}. \quad (5)$$

Equation (2) may be written as

$$Q_{\text{solution}}=Ww(T)(p_0\exp\left[-U_0/kT\right]+p_1\exp\left[-U_1/kT\right]+\cdots). \quad (6)$$

This may be rewritten as

$$Q_{\text{solution}}=Ww(T)p_0\exp\left[-U_0/kT\right]\times(1+p_1/p_0\exp\left[-(U_1-U_0)/kT\right]+\cdots). \quad (7)$$

[10] R. H. Fowler, *Statistical Mechanics* (Cambridge University Press, Cambridge, 1929), p. 117.

Another way of writing (7) is

$$Q_{\text{solution}}=Q'(T)\exp\left[-U_a/kT\right], \quad (8)$$

where $U_0=U_a$ and $Q'(T)$ contains the rest of the expression. Likewise (4) may be written

$$Q_{\text{silica}}=Q''(T)\exp\left[-(U_m+z\epsilon\zeta)/kT\right]. \quad (9)$$

Rewriting (5), one obtains

$$\frac{n}{W}=\frac{Q'(T)\exp\left(-U_a/kT\right)}{Q''(T)\exp\left[-(U_m+z\epsilon\zeta)/kT\right]}, \quad (10)$$

where n/W is, for all practical purposes, the concentration of the anions in solution.

From (10), it is immediate that

$$kT\left\{\ln c-\ln\frac{Q'(T)}{Q''(T)}\right\}=z\epsilon\zeta+(U_m-U_a). \quad (11)$$

Equation (11) is derived by assuming that each water molecule is available as a potential equilibrium position for an adsorbed anion. However, each anion in solution puts out of action, say q water molecules, and, consequently, the number of water molecules available as equilibrium positions is $(W-qn)$, and (11) takes a more rigorous form and becomes

$$\zeta=\frac{\bar{U}_a-\bar{U}_m}{zF}+\frac{RT}{zF}\ln\left\{\frac{c}{1-qc}\frac{Q'(T)}{Q''(T)}\right\}, \quad (12)$$

where $\bar{U}_a$ and $\bar{U}_m$ are molar quantities instead of the molecular quantities in (11); R is the molar gas constant, and F is the Faraday constant. For this type of model, Fowler suggests that $Q'(T)/Q''(T)$ is very nearly unity, but need not be for a more general model. Consequently a simplification of (12) yields the approximate formula for the ζ-potential

$$\zeta=\frac{\bar{U}_a-\bar{U}_m}{zF}+\frac{RT}{zF}\ln c. \quad (13)$$

COMPARISON WITH EXPERIMENT

In calculating the zeta-potential from streaming potential data, one uses the formula,

$$\zeta=(4\pi\eta/D)(\kappa E/P), \quad (14)$$

and from electro-endosmosis,

$$\zeta=(4\pi\eta/D)(l/E), \quad (15)$$

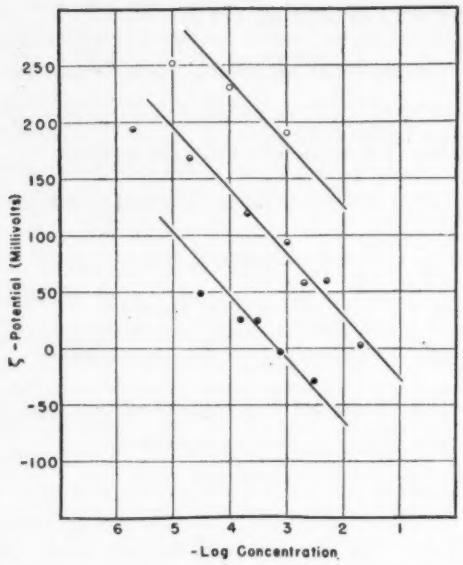

FIG. 1. The newly defined zeta-potential (1.7 times the conventional values) *versus* concentration. The points represent the data of Jones, Wood, and Robinson; the solid lines give the slope of the lines in the proposed theory. Potassium chloride, ○; barium chloride, ◒; lanthanum chloride, ●.

where D is the dielectric constant of the electric double layer, η is the viscosity coefficient of the liquid in the double layer, κ is the specific conductance of the solution in the capillary tube, l is the length of the capillary, P is the pressure, and E is the measured potential. In both cases all of the quantities are measured except η and D. These are, in general, taken as the same as for pure water. Some authors[11] have pointed out that this assumption may be in error, especially in connection with the dielectric constant. Consequently, the values of the zeta-potential (Helmholtz-Perrin) as calculated are probably erroneous because of the uncertainty in the value of the dielectric constant. Thus, exact agreement between this theory and the data of Jones, Wood, Robinson, Rutgers, and deSmet is not expected. The dipole moment per unit area of the electrical double layer is the quantity actually measured by the experiments, and further assumptions must be made in order to convert the moment into potential. However, one should expect the slopes of the lines representing the experimental data to be the same for the various salts. Such was actually observed for most of the salts.

A formula similar to (13) was proposed by Rutgers and deSmet in which C referred to the concentration of the *cation*, in contrast to the C of (11) and (13) in this article which refers to the *anion* concentration. Their data, with divalent cations, was practically the same as that reported by Wood and Robinson.[7] The factor $2.303\ RT/zF$ gives a slope of 29 mv for the $\zeta - \log C$ curve in agreement with both groups of investigators. If C in (13) referred to the concentration of the cation, then one would expect the slope of the curve for the uni-univalent electrolytes to be greater than any of the others. Previously, Rutgers and Verlende[1] had derived the formula, and their last statement in the article is precisely: ". . . für 1–1, 2–1, 3–1, 4–1-wertige Elektrolyten sind die $\zeta - \log C$ Kurven also Geraden, deren Neigung bzw. 58, 29, 19.3 und 14.5 mV. beträgt." But the above assertion was not substantiated by either Rutgers and co-workers or Jones, Wood, and Robinson.

This writer believes that the slope of 29 mv (actually about 34 mv by Wood and Robinson) bears no relation to the factor $2.303\ RT/2F$. The theory proposed in this article makes the slope of each line about 58 mv. Therefore, it is proposed that the data should be multiplied by a factor of about 1.7. This proposal means that the dielectric constant (or the ratio of D to η) for the electric double layer is only 0.6 that of the value for pure water. This assertion could be tested experimentally by determining the number of ions at the surface (not adsorbed on the surface) from surface conductance measurements. Verification of the theory would result if the number of ions calculated in this manner would be about five times the number calculated from the Helmholtz-Perrin zeta-potential.

A graph is given of the newly defined zeta-potential (1.7 times the Helmholtz-Perrin zeta-potential) *versus* concentration (see Fig. 1). The value for water is greater than that of any of the salts.[12]

[11] H. B. Bull and R. A. Gortner, Physics **2**, 21 (1932); J. W. McBain and M. E. L. McBain, Zeits. f. physik. Chemie **161**, 279 (1932); E. A. Guggenheim, Trans. Faraday Soc. **36**, 5 (1940); L. A. Wood, J. Am. Chem. Soc. **68**, 432 (1946).

[12] L. A. Wood, J. Am. Chem. Soc. **68**, 437 (1946).

THE JOURNAL OF CEHMICAL PHYSICS VOLUME 14, NUMBER 12 DECEMBER, 1946

Absorption of Water by Films of Cellophane and Polyvinyl Alcohol

E. CREUTZ* AND ROBERT R. WILSON**
*Princeton University,*** *Princeton, New Jersey*

(Received September 11, 1946)

The absorption of water and dehydration of these films is found to obey a diffusion equation by means of which a diffusivity may be defined. This is not a constant but depends on the water concentration in the foils. A rapid change in water content immediately after changing the ambient conditions suggests the presence of adsorbed surface layers. The total absorption is found to increase faster than the relative humidity.

INTRODUCTION

FOR experiments on scattering of high energy protons by hydrogen carried out by the authors at Princeton University in 1941 it was decided to use pure Cellophane as a scattering foil. In order to obtain the absolute value of the scattering cross section it was necessary to know accurately the percentage of hydrogen by weight in the foils. Very pure Cellophane was prepared for us by Dr. Nelson Allen of the Cellophane Analytical Research Division of DuPont. This eliminated the uncertainty due to small amounts of glycerine usually added to this material. However the Cellophane was found to absorb amounts of water depending upon the relative humidity of the atmosphere and it was necessary to understand this phenomenon quantitatively in order to know the true hydrogen content of the material.

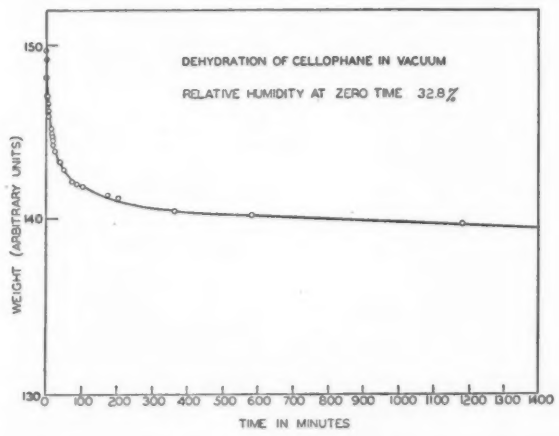
DEHYDRATION OF CELLOPHANE IN VACUUM
RELATIVE HUMIDITY AT ZERO TIME 32.8%
WEIGHT (ARBITRARY UNITS)
150
140
130
0 100 200 300 400 500 600 700 800 900 1000 1100 1200 1300 1400
TIME IN MINUTES

FIG. 1. Weight of $\frac{1}{2}''$ diameter Cellophane foil .0005" thick as a function of time it was left in vacuum after having been intially in equilibrium with air of relative humidity 32.8 percent.

METHOD AND RESULTS

Disks of the foil $\frac{1}{2}''$ in diameter (1.27 cm² in area) were punched with a special tool from a sheet placed between clean paper. These were handled with tweezers and weighed in a quartz fiber microbalance built along the lines of that described by Strong[1] and put in a chamber which could be evacuated.

The rate of dehydration of the foil in vacuum was investigated as well as the rate at which it picked up water again when air of a known relative humidity was re-admitted to the balance

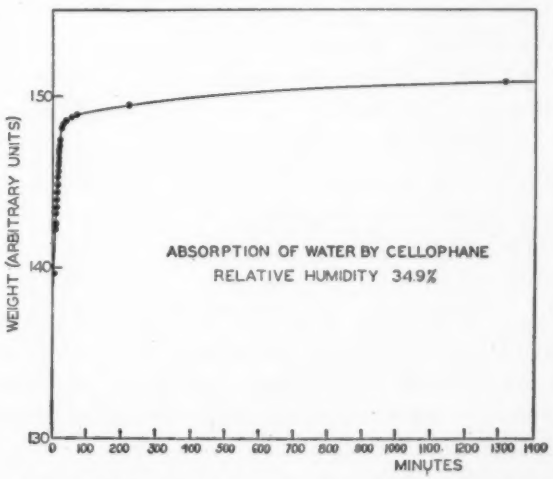

FIG. 2. Weight of Cellophane foil as a function of time after having been immersed in air of relative humidity 34.9 percent. Foil was initially in vacuum.

* Now at Carnegie Institute of Technology, Pittsburgh, Pennsylvania.

** Now at Harvard University, Cambridge, Massachusetts.

*** This work was done in 1940 but not published because of war work.

[1] Strong, *Procedures in Experimental Physics* (Prentice-Hall, Inc., New York, 1942), p. 215.

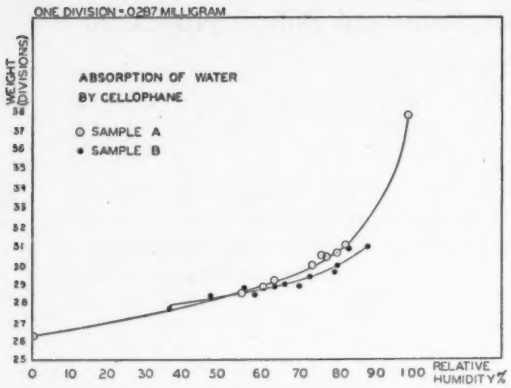

FIG. 3. Weight of .0001" Cellophane foils in equilibrium with air of various relative humidities.

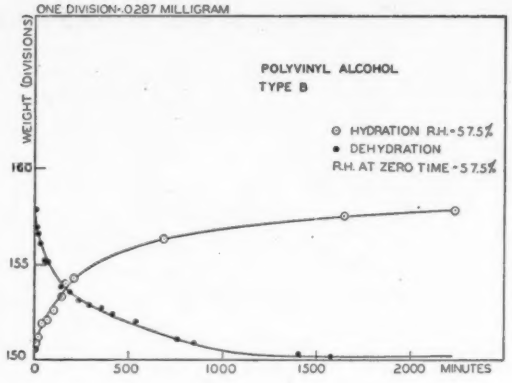

FIG. 4. Weight of ½" diameter foil of polyvinyl alcohol type *B* during dehydration, and hydration, in air of relative humidity 57.5 percent.

chamber. Relative humidities were measured with a sling hygrometer.

Figure 1 shows the weight of a Cellophane foil about .0005 inch thick as a function of the time it was left in the evacuated chamber after having been initially in equilibrium with air at 32.8 percent relative humidity at approximately 30°C. The total loss in weight after 20 hours when the weight had become constant was 0.264 mg or 0.208 mg per square centimeter.

Figure 2 shows the weight of the Cellophane as a function of time after air of relative humidity 34.9 percent had been admitted to the chamber. In this case the total gain in weight was larger than the initial loss as expected since the air was now of higher relative humidity.

Figure 3 shows the weight of two different samples of Cellophane about 0.0001 inch thick as a function of relative humidity of the air with which they are in equilibrium. For these thinner foils equilibrium was reached in about two hours. Only one reading was taken in a day allowing sufficient time for the foil to reach a steady state at the particular value of the humidity which existed. The point at 100 percent was taken by placing a dish of water inside the balance chamber and sealing it up. In this case the weight gain was 0.336 mg.

Figure 4 shows the weight loss in vacuum of polyvinyl alcohol film type *B* after standing in air of relative humidity 57.5 percent and the regain of weight when the air was re-admitted. Weight change was 0.217 mg.

DISCUSSION[2]

The diffusion of moisture into and out of the foil might be expected to follow the equation

$$h^2(d^2M/dx^2) = dM/dt, \tag{1}$$

where M is the concentration of water in the foil in grams per cm³, x is measured along the thickness of the foil, t is the time, and h^2 is the diffusivity. Since the diameter of the foil is large compared to the thickness, it may be treated as an infinite slab. The boundary conditions for the case of dehydration when the foil whose surfaces are in the planes $x=0$ and $x=L$, is placed in vacuum, are as follows:

$$\begin{aligned} &M=M_0, \quad 0<x<L \text{ for } t=0, \\ &M=0, \quad x=0 \text{ or } L, \quad \text{for all } t, \end{aligned} \tag{2}$$

the general solution of Eq. (1),[3]

$$M = A \exp(-h^2\gamma^2 t) \begin{matrix}(\sin \gamma x) \\ (\cos \gamma x)\end{matrix} \tag{3}$$

then becomes:

$$M = M_0 - \frac{4}{\pi}\sum_{n=0}^{\infty} \frac{1}{2n+1} \exp\left[-\left\{\frac{h^2\pi^2 t(2n+1)^2}{L^2}\right\}\right] \times \sin \pi x\left[\frac{(2n+1)}{L}\right], \tag{4}$$

to fit the boundary conditions for dehydration.

[2] For an excellent general discussion of this problem see R. M. Barrer, *Diffusion in and through Solids* (Cambridge University Press, New York, 1941).

[3] Ingersoll and Zobel, *Mathematical Theory of Heat Conduction* (Ginn and Company, 1913), p. 105.

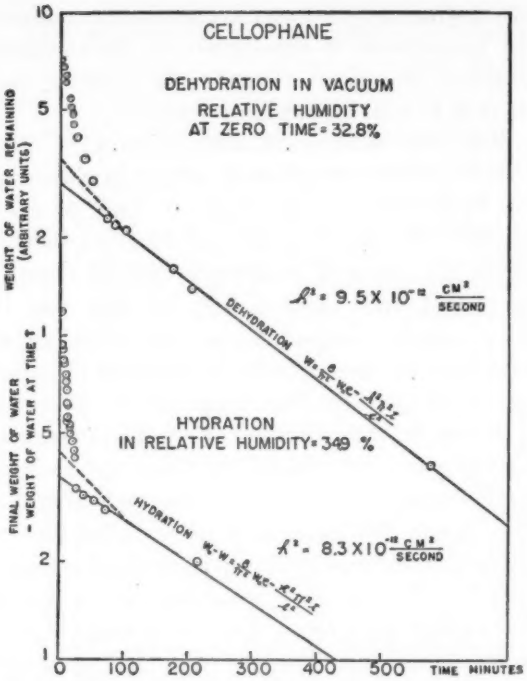

FIG. 5. Semi-logarithmic plots of weight of Cellophane foil during dehydration in vacuum and rehydration in air. The diffusivities, h^2, are computed from the straight parts of the curves at times greater than 50 minutes. The ordinate of the lower curve is the final weight of water (after many hours) minus the weight of water at the time indicated by the abscissa. This number is larger than the corresponding ordinate for the upper curve because the final weight corresponds to 34.9 percent relative humidity rather than 32.8 percent which was the initial value in the case of dehydration.

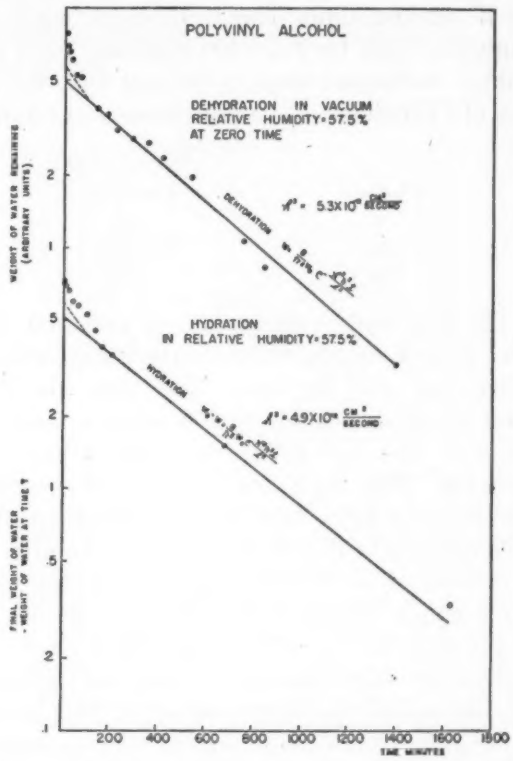

FIG. 6. Semi-logarithmic plots of weight of polyvinyl alcohol films during dehydration and hydration. The diffusivities, h^2, are computed from the straight parts of the curves at times greater than 100 minutes. The lower curve shows the final weight of water (after many hours), minus the weight at the time indicated by the abscissa.

For the case when moist air is again let into the chamber around the dry foil, the boundary conditions are

$$\begin{aligned} &M = M_0, \quad x = 0 \text{ or } L, \quad \text{for all } t, \\ &M = 0, \quad 0 < x < L, \quad \text{for } t = 0. \end{aligned} \tag{5}$$

The solution then is

$$M = M_0 \left\{ 1 - \frac{4}{\pi} \sum_{n=0}^{\infty} \frac{1}{2n+1} \times \exp\left[-\frac{h^2 \pi^2 t (2n+1)^2}{L^2} \right] \sin \pi x \frac{(2n+1)}{L} \right\}. \tag{6}$$

For comparison with the experiment we wish to know the total amount of moisture in the foil at any time or

$$W = \text{area} \cdot \int_0^L M dx. \tag{7}$$

For the case of dehydration this is, integrating Eq. (4) term by term,

$$W = W_0 \frac{8}{\pi^2} \sum_{n=0}^{\infty} \times \left\{ \exp\left[-\left\{ \frac{h^2 \pi^2 t}{L^2} (2n+1)^2 \right\} \right] \frac{1}{(2n+1)^2} \right\} \tag{8}$$

where W_0 is the initial total weight of moisture.

For dehydration, integrating Eq. (6) gives

$$W = W_0 \left(1 - \frac{8}{\pi^2} \sum_{n=0}^{\infty} \times \exp\left[-\left\{ \frac{h^2 \pi^2 t}{L^2} (2n+1)^2 \right\} \right] \frac{1}{(2n+1)^2} \right). \tag{9}$$

For large values of time t, terms with $n > 0$ may be neglected and the diffusivity h^2 may be found from the slope of the experimental plot of

log W against time. The terms with $n>0$ are important only for $t<\sim 100$ minutes. Thus the ratio of the second term to the first term for the case of Cellophane for various times is as follows:

T (min.)	Second term / First term
0	1/9
50	0.023
100	0.005

The first term is 81 percent of the total sum even at $t=0$. An approximation to the theoretical curve may thus be made using only the first term of the series for $t>100$ minutes and increasing this by 19 percent$\times(1-t/100)$ for $t>\sim 100$. This gives too large a value to the sum for $t<\sim 100$ except at $t=0$. This correction is shown by the dotted lines in Figs. 5 and 6.

It is seen from the semi-logarithmic plots that (1) a single exponential term gives a good fit to the data for $t>\sim 50$ minutes for Cellophane and for $t>\sim 100$ minutes for polyvinyl alcohol; (2) increasing the single term by 19 percent $\times(1-t/100)$ to correct for all the remaining terms at values of $t>100$ (theoretically too large a correction except for $t=0$) does not give values on the dehydration curve as large as the experimental ones at small t.

The second fact noted above has led us to conclude (a) the diffusivity h^2 of water in these substances is not a constant but increases as the water content increases and (b) there is water absorbed on the surface of the foil in layers 100 or more molecules thick. This can account for part of the large deviation of the experimental data from straight exponential plots in the case of dehydration. Another effect noticed was that the weight gain when the foil is in equilibrium with air of various relative humidities is not linear but increases faster than the relative humidity. This is in agreement with the hypothesis of Peirce[4] of alpha- and beta-water in cotton where alpha-water is chemically combined and beta-water is condensed at high relative humidity in spaces between the hexose units where it is held by capillary forces.

That the increase of diffusivity with water content cannot be the only effect is shown by the hydration curves Figs. 5 and 6 where log (W_0-W) has been plotted. At small t these curves also are seen to deviate upward from the theoretical lines even though in this case the water content is increasing with time so the diffusivity should initially be small if the above conclusion is true. This deviation we believe to be caused by surface absorption. To account for the observed differences between the extrapolated dotted lines and the observed weight at $t=0$, about 100 molecular layers would be required in the case of polyvinyl alcohol and about 2000 in the case of Cellophane, assuming the true surface area to be just the geometric value for a smooth disk. Actually the effective surface may be much larger due to irregularities of the order of molecular dimensions. Schiff[5] has shown that adsorbed surface layers of the order of 100 molecules thick can be accounted for by Van der Waals' forces in the special case of helium II.

The opposite effect, namely initial rapid evaporation of absorbed surface water in the case of dehydration would tend to make those curves too steep initially, so the effect of the change of h^2 is less pronounced than at first apparent from the initial part of dehydration curves. The real change of h^2 should tend to make the average slope of the hydration curves steeper than that of the dehydration curves at times from 100 to 500 minutes, since the foil is dryer in the case of dehydration and the average diffusivity will be smaller. This effect is apparently smaller than the accuracy of the data resulting from the subtraction required to obtain the hydration curves (Figs. 5 and 6).

[4] Peirce, J. Text. Inst. (T) **20**, 133 (1929).

[5] L. I. Schiff, Phys. Rev. **59**, 839 (1941).

THE JOURNAL OF CHEMICAL PHYSICS VOLUME 14, NUMBER 12 DECEMBER, 1946

Thermodynamic Properties of Gaseous Boron Trifluoride, Boron Trichloride, and Boron Tribromide

HUGH M. SPENCER
Cobb Chemical Laboratory, University of Virginia, Charlottesville, Virginia
(Received September 25, 1946)

In this paper are presented tables of the thermodynamic functions heat content, free energy, entropy, and heat capacity of boron trifluoride, boron trichloride, and boron tribromide in the ideal gas state at 1 atmosphere from 298.16° to 1000°K. These functions were calculated from Raman and infra-red spectra in the case of the two first mentioned and from the Raman spectrum of liquid boron tribromide. A satisfactory calorimetric check of the entropy of boron trifluoride is presented.

I. INTRODUCTION

IN recent years much interest has been shown in the formation of addition compounds with the boron trihalides and the use of the trihalides, particularly of boron trifluoride, as catalysts, as is witnessed by the reviews of Kästner[1] and the series of papers by G. F. Hennion in the *Journal of the American Chemical Society*. These compounds have passed from academic to industrial interest.

The spectroscopic and molecular data (Part II) are sufficiently complete to permit the calculations of the thermodynamic functions of boron trifluoride, boron trichloride, and boron tribromide to the rigid rotator, harmonic oscillator approximation with some increase of uncertainty in that order (Part III). Low temperature calorimetric measurements and vapor pressure data permit a check of the entropy of boron trifluoride (Part IV).

The following physical constants and chemical atomic weights were used in the calculations:

$R = 1.98718$ cal. deg.$^{-1}$ mole^{-1},
$hc/k = 1.43847$ cm deg.,
$N = 6.02283 \times 10^{23}$ mole^{-1},
Atomic weight of $^{11}B = 11.00992$,
Atomic weight of $^{10}B = 10.01361$,
Atomic weight of equilibrium B = 10.82.

The constants are those selected by Wagman, Kilpatrick, Taylor, Pitzer, and Rossini.[2] The chemical atomic weights of boron of masses 10 and 11 are derived from the physical atomic weights: $^{11}B = 11.01292$ and $^{10}B = 10.01631$ of Bainbridge and Jordan as reported by Livingston and Bethe[3] and the ratio of the physical to the chemical atomic scale, 1.000272.

Recently Ingraham[4] has satisfactorily determined the percentage abundance of the boron isotopes. His values of 81.17 percent for ^{11}B and 18.83 percent for ^{10}B and the chemical atomic weights of the isotopes yields 10.822 for equilibrium boron as compared to 10.82 of the international atomic weights.

II. SPECTROSCOPIC AND MOLECULAR DATA

The spectroscopic data for boron trifluoride include the infra-red spectra of Bailey, Hale, and Thompson[5] and of Gage and Barker[6] and the Raman spectrum of the vapor by Anderson, Lassettre, and Yost[7a] and by Yost, DeVault, Anderson, and Lassettre.[7b] Herzberg[8] has summarized these data and shown that they are in agreement with the plane symmetrical model (point group D_{3h}). This is also in agreement with the zero dipole moment and the electron diffraction measurements. The latter by Lévy and Brockway[9] fix the B−F distance as 1.30±0.02A. From the study of the fine structure of the

[1] B. Kästner, Zeits. f. angew. Chemie **54**, 273, 296 (1941).
[2] D. D. Wagman, J. E. Kilpatrick, W. J. Taylor, K. S. Pitzer, and F. D. Rossini, J. Research Nat. Bur. Stand. **34**, 143 (1945).
[3] M. S. Livingston and H. A. Bethe, Rev. Mod. Phys. **9**, 245 (1937).
[4] M. G. Ingraham, Phys. Rev. **70**, 119 (1946).
[5] C. R. Bailey, J. B. Hale, and J. W. Thompson, Proc. Roy. Soc. (London) **A161**, 107 (1937).
[6] D. M. Gage and E. F. Barker, J. Chem. Phys. **7**, 455 (1939).
[7a] T. F. Anderson, E. N. Lassettre, and D. M. Yost, J. Chem. Phys. **4**, 703 (1936); [b] D. M. Yost, D. DeVault, T. F. Anderson, and E. N. Lassettre, *ibid.*, **6**, 424 (1938).
[8] G. Herzberg, *Infrared and Raman Spectra of Polyatomic Molecules* (D. Van Nostrand Company, Inc., New York, 1945), pp. 298–9.
[9] H. A. Lévy and L. O. Brockway, J. Am. Chem. Soc. **59**, 2085 (1937).

TABLE I. Heat content, free energy, entropy, and heat capacity of boron trifluoride in the ideal gas state at 1 atmosphere. Molecular weight = 67.82. $\sigma = 6$. $I_2 = I_3 = 78.8_4 \times 10^{-40}$, $I_1 = 157.7 \times 10^{-40}$ g cm².

T°K	$\frac{H^0 - H_0^0}{T}$	$\frac{-(F^0 - H_0^0)}{T}$	S^0	Cp^0
	cal deg.$^{-1}$ mole^{-1}			
298.16	9.338	51.357	60.695	12.063
300	9.355	51.414	60.770	12.094
350	9.811	52.892	62.702	12.981
400	10.257	54.230	64.488	13.764
450	10.686	55.464	66.150	14.454
500	11.094	56.611	67.704	15.059
600	11.841	58.70	70.54	16.046
700	12.497	60.58	73.07	16.792
800	13.071	62.29	75.36	17.358
900	13.572	63.85	77.42	17.792
1000	14.012	65.31	79.32	18.128

parallel ν_2 band ($\Delta\nu = 0.71$ cm^{-1}), Gage and Barker determined this distance to be 1.29A. This value leads to $I_2 = I_3 = 78.8_4 \times 10^{-40}$ and $I_1 = 157.7 \times 10^{-40}$ g cm².

The Raman spectrum of liquid boron trichloride has been studied by Venkateswaran[10]; Anderson, Lassettre, and Yost[7a]; and Wagner.[11] The latter author confirmed the measurements of Anderson, Lassettre, and Yost and with greater dispersion found three of the four possible lines caused by the chlorine isotopic splitting of the symmetric valence vibration, ν_1, in approximately the separations and intensities to be expected. Anderson, Lassettre, and Yost's assignment of the fundamental frequencies is as follows: $\nu_1 = 471$; $2\nu_2 = 902(^{11}BCl_3)$; $\nu_3(2) = 946(^{11}BCl_3)$, $= 989(^{10}BCl_3)$; and $\nu_4(2) = 253$ cm^{-1}.[12] They also made a more plausible assignment of the fundamental frequencies for the infra-red absorption spectrum of boron trichloride vapor, based upon the data of Cassie,[13] as follows: $\nu_1 = 471$; $\nu_2 = 462(^{11}BCl_3)$; $\nu_3(2) = 958(^{11}BCl_3)$, $= 996(^{10}BCl_3)$; $\nu_4(2) = 243$ cm^{-1}. The dispersion of Cassie's measurements was insufficient to permit the determination of the fine structure. Lévy and Brockway's measurement[9] of the B−Cl distance, 1.73±0.02A, yields $I_2 = I_3 = 264._3 \times 10^{-40}$ and $I_1 = 528._6 \times 10^{-40}$ g cm².

[10] S. Venkateswaran, Ind. J. Phys. **6**, 275 (1931).
[11] J. Wagner, Zeits. f. physik. Chemie **193**, 55 (1943).
[12] The totally symmetric vibration ν_1, involving motion of the halogen atoms, is independent of the mass of the boron isotope. For the doubly degenerate ν_4 the isotope effect, which should be small, has not been observed in the cases of boron trichloride and boron tribromide.
[13] A. B. D. Cassie, Proc. Roy. Soc. (London) **A148**, 87 (1935).

For boron tribromide there are no infra-red measurements and the Raman spectrum studies have been made with the liquid.[7a, 11, 14] Though the later measurements of Wagner give the frequencies $\nu_1 \cdots \nu_4$, less than those of Anderson, Lassettre, and Yost by 2, 2, 6, and 1 cm^{-1}, respectively, those of Anderson, Lassettre, and Yost have been accepted. They are $\nu_1 = 279$, $\nu_2 = 372(^{11}BBr_3)$, $\nu_3(2) = 806(^{11}BBr_3)$, $= 846(^{10}BBr_3)$ and $\nu_4(2) = 151$ cm^{-1}. Lévy and Brockway's measurement of the B−Br distance, 1.87±0.02A, yields $I_2 = I_3 = 696 \times 10^{-40}$ and $I_1 = 1392 \times 10^{-40}$ g cm².

According to the Teller-Redlich product rule, for such isotopic molecules as $^{11}BX_3$ and $^{10}BX_3$, the product of the ratios of the frequencies for all vibrations of a given symmetry type is equal to the square root of the ratio of the reciprocal mean masses, i.e.,

$$\frac{\nu_2(^{10}BX_3)}{\nu_2(^{11}BX_3)} = \frac{\nu_3\nu_4(^{10}BX_3)}{\nu_3\nu_4(^{11}BX_3)} = \left[\frac{\mu(^{11}BX_3)}{\mu(^{10}BX_3)}\right]^{\frac{1}{2}}.$$

The ν_2's for boron trifluoride are in excellent agreement with this rule and $\nu_3\nu_4$ values agree satisfactorily.[8] For boron trichloride and boron tribromide for which $(\mu_{11}/\mu_{10})^{\frac{1}{2}}$ is 1.0441 and 1.0466, respectively, direct experimental test of this rule is not possible, since the ν_2's for $^{10}BX_3$ have not been measured and the ν_4's have not been resolved. The calculated values of the ν_2's given by Anderson, Lassettre, and Yost[7a] are not quite in accord with these ratios. For the present calculations the Teller-Redlich rule and the ν_i values for $^{11}BX_3$ have been accepted and values for $^{10}BX_3$ have been calculated. The former multiplied by the abundance fraction 0.8117 and the latter by 0.1883 yield for the equilibrium BX_3:

	ν_1	ν_2	$\nu_3(2)$	$\nu_4(2)$
$BCl_3(g)$	471	465.8	965.2	243.2 cm^{-1}
$BBr_3(l)$	279	375.3	812.0	151.2

III. THERMODYNAMIC FUNCTIONS

The frequencies given above for boron trichloride and boron tribromide, and ones calculated from Table 75 of reference 8 by combination in the relative proportions of 0.8117 and

[14] R. Ananthakrishnan, Proc. Indian Acad. Sci. **A4**, 74 (1936).

0.1883, have been used with the moments of inertia mentioned in Section II to calculate the thermodynamic functions of the three trihalides. The symmetry number, σ, is 6. Nuclear spins and the effect of isotopic mixing have been neglected. The values of the heat content, free energy, entropy, and heat capacity of boron trifluoride, boron trichloride, and boron tribromide in the ideal gas state at 1 atmosphere are summarized in Tables I–III. The precision of expression of the free energy and entropy does not reflect the uncertainty in the B−X distances. Thus, e.g., if r_{B-X} were greater by 0.01A in each case, i.e., equal to the electron diffraction value for boron trifluoride, their values would be greater by 0.043, 0.034, and 0.033 cal. deg.$^{-1}$ mole^{-1}, respectively.

IV. CALORIMETRIC AND OTHER COMPARISONS

Eucken and Schröder[15] measured the heat capacities, heats of transition and fusion of boron trifluoride from 12° to 173°K, approximately the boiling point. The boiling point has been variously reported as −99.9 to −101°C.[16] Eucken and Schröder obtained the entropy of liquid boron trifluoride at 154.5°K from their calorimetric data. They combined this with a value of the entropy of vaporization at 154.5° and the saturation pressure, derived from the vapor pressure data and equation of Pohland and Harlos,[17] and with the entropy of compression to 1 atmosphere to obtain the entropy in the ideal gas state at 1 atmosphere and 154.5°K. The entropy change, $S^0_{298.2} - S^0_{154.5}$, for the vapor was obtained from values of the characteristic temperatures of the fundamental vibrations supposedly based on the results of Yost, DeVault, Anderson, and Lassettre.[7b] Their result for the entropy in the ideal gas state at 1 atmosphere and 298.2°K was 61.17 cal. deg.$^{-1}$ mole^{-1}.

TABLE II. Heat content, free energy, entropy, and heat capacity of boron trichloride in the ideal gaseous state at one atmosphere. Molecular weight = 117.911. $\sigma = 6$. $I_2 = I_3 = 264.3 \times 10^{-40}$, $I_1 = 528.6 \times 10^{-40}$ g cm^2.

T°K	$\frac{H^0 - H_0^0}{T}$	$\frac{-(F^0 - H_0^0)}{T}$	S^0	Cp^0
	cal. deg.$^{-1}$ mole^{-1}			
298.16	11.262	58.03	69.29	14.97
300	11.284	58.10	69.38	15.00
350	11.873	59.88	71.75	15.79
400	12.415	61.51	73.93	16.43
450	12.879	62.99	75.87	16.94
500	13.306	64.37	77.68	17.36
600	14.04	66.86	80.90	17.99
700	14.63	69.08	83.71	18.42
800	15.13	71.06	86.19	18.72
900	15.54	72.87	88.41	18.94
1000	15.89	74.52	90.41	19.10

TABLE III. Heat content, free energy, entropy, and heat capacity of boron tribromide in the ideal gaseous state at 1 atmosphere. Molecular weight = 250.568. $\sigma = 6$. $I_2 = I_3 = 696 \times 10^{-40}$, $I_1 = 1392 \times 10^{-40}$ g cm^2.

T°K	$\frac{H^0 - H_0^0}{T}$	$\frac{-(F^0 - H_0^0)}{T}$	S^0	Cp^0
	cal. deg.$^{-1}$ mole^{-1}			
298.16	12.609	64.88	77.49	16.25
300	12.631	64.96	77.59	16.28
350	13.187	66.97	80.16	16.88
400	13.695	68.75	82.44	17.41
450	14.130	70.39	84.52	17.80
500	14.514	71.89	86.41	18.10
600	15.16	74.60	89.76	18.58
700	15.67	76.98	92.64	18.88
800	16.08	79.10	95.18	19.10
900	16.43	81.01	97.44	19.25
1000	16.72	82.76	99.47	19.37

The calculations of Eucken and Schröder are subject to several minor and two major objections. Two of their graphically determined areas are in error by approximately 0.1 cal. deg.$^{-1}$ mole^{-1}. Inconsistent (and incorrect) values of hc/k appear to have been used in obtaining the characteristic temperatures. More important is the fact that no corrections for non-ideality appear to have been made in determining the heat of vaporization. The other major objection concerns their use of 1.13 cal. deg.$^{-1}$ mole^{-1} as the entropy change involved in going from 142.15° to 144.46°K, which purports to be that involved in the transition and

$$\int_{142.15}^{144.46} Cp \cdot d \ln T.$$

According to their Table 4 the energy input per mole in increasing the temperature 1.128° (including the transition) was 61.0 cal., the contribution of the normal molal heat was 42.6 cal., leaving 18.4 (given as *ca.* 18) as the true heat of

[15] A. Eucken and E. Schröder, Zeits. f. physik. Chemie **B41**, 307 (1938).

[16] Landolt-Börnstein, *Tabellen*, third edition, Vol. I, p. 338; Supplement III, p. 318.

[17] E. Pohland and W. Harlos, Zeits. f. anorg. allgem. Chemie **207**, 242 (1932).

TABLE IV. Summary of the calculation of the entropy of boron trifluoride in the ideal gas state at 298.16°K and 1 atmosphere, based on calorimetric and vapor pressure data to 154.5°K and statistically calculated ΔS^0 from 154.5 to 298.16°K.

	cal. deg.$^{-1}$ mole^{-1}
Extrapolation, 0–12.6°K	0.55
Graphical, solid II, 12.6–142.15°K	18.42
Transition and $\int_{142.15}^{144.45} Cp(\text{solid I}) d \ln T$	0.74
Fusion, 1014/144.46	7.02
Graphical, liquid, 144.46–154.5°K	1.65
Vaporization at 154.5°K, $p=0.2185$ atmos.	28.55
Correction for gas imperfection	0.04
Entropy of ideal gas at 154.5°K and $p=0.2185$ atmos.	56.97
Compression to 1 atmos.	−3.02
Entropy of ideal gas at 154.5°K and $p=1$ atmos.	53.95
$S^0_{298.16}-S^0_{154.5}$	6.85
Entropy of ideal gas at 298.16°K and $p=1$ atmos.	60.80

transition. This indicates an average heat capacity in this narrow region of 37.8 cal. deg.$^{-1}$ mole^{-1}. This is in qualitative agreement with their statement: "In this region the heat capacity was abnormally high (the minimum value was ~35 cal. deg.$^{-1}$ mole^{-1})." It would appear that the entropy change in going from 142.15° to 144.46°K should be 0.74 cal. deg.$^{-1}$ mole^{-1}.

Kelley[18] recalculated the entropy of boron trifluoride in essentially the same manner, but with satisfactory graphical areas. His result was $S^0_{298.1}=61.4$ cal. deg.$^{-1}$ mole^{-1}.

Pohland and Harlos[17] determined the vapor pressure of liquid boron trifluoride at thirteen temperatures in the range 145.9° to 170.3°K. Their equation

$$\log p \text{ (in mm Hg)} = -1174.4/T+1.75 \log T -0.013350T+8.0536$$

is a fair representation of their data, $\sum(p_{\text{obs.}}-p_{\text{calcd.}})$ for six positive and seven negative deviations totaling 5 and 7 mm, respectively. Four values in the range 187.5 to 653 mm by Fischer and Weidemann[19] are in good agreement with the equation of Pohland and Harlos. Other measurements extant in this pressure range[20] do not merit equal consideration since the samples were not pure or the measurements were made with insufficient accuracy.

If one uses the equation of Pohland and Harlos, with the assumption that the vapor obeys the approximate Berthelot equation of state in the region concerned

$$\Delta H_{\text{vap}} = RT^2 \frac{d \ln p}{dT}\left[1+\frac{9}{128}\frac{pT_c}{p_cT}\left(1-\frac{pT_c^2}{T^2}\right)-\frac{pV_{\text{liq}}}{RT}\right],$$

where $p_c=49.2$ atmos., $t_c=-12.25$°C,[21] and $\rho(\text{liquid})=2.25-0.003928T$, based on Fischer and Weidemann's data, the heat of vaporization at the temperature and pressure used by Eucken and Schröder and by Kelley is 4411 cal. mole^{-1}, and $\Delta S(\text{vap.})=29.55$ cal. deg.$^{-1}$ mole^{-1}. This replaces 28.68 and 28.74 given by Eucken and Schröder and Kelley, respectively.

The recalculation of the entropy of boron trifluoride in the ideal gas state at 298.16°K and 1 atmosphere is summarized in Table IV. For the present calculations the entropy change $S^0_{298.16}-S^0_{154.5}$ was obtained from the values of $S^0_{298.16}$ and $S^0_{154.5}$ derived from the spectroscopic data, rather than by an integration of calculated heat capacities in the region.

Similar calculations at each of the nine intermediate temperatures at which Pohland and Harlos measured the vapor pressure (i.e., excluding the three lowest and one highest temperatures) gave $S^0_{298.16}=60.69$ (average) cal. deg.$^{-1}$ mole^{-1}, with six positive deviations totaling 0.37 and three negative deviations totaling 0.39. The agreement with the statistically calculated value of Table I, 60.70, is excellent. Eucken and Schröder and Kelley's statistically calculated values were 61.11 and 61.4 cal. deg.$^{-1}$ mole^{-1}, respectively.

The entropies of boron trichloride and boron tribromide calculated from the spectroscopic data by Kelley,[18] 68.6 and 76.7 cal. deg.$^{-1}$ mole^{-1}, respectively, are in error as a result of the use of the harmonic $2\nu_2$ in place of the fundamental ν_2.

[18] K. K. Kelley, U. S. Bur. Mines, Bull. No. 434 (1941).
[19] W. Fischer and W. Weidemann, Zeits. f. anorg. allgem. Chemie **213**, 106 (1933).
[20] O. Ruff *et al.*, Zeits. f. anorg. allgem. Chemie **206**, 59 (1932); L. LeBoucher and W. Fischer with W. Biltz, *ibid.*, **207**, 61 (1932).
[21] H. S. Booth and J. M. Carter, J. Phys. Chem. **36**, 1359 (1932).

THE JOURNAL OF CHEMICAL PHYSICS VOLUME 14, NUMBER 12 DECEMBER, 1946

The Theory of the Racemization of Optically Active Derivatives of Diphenyl

F. H. WESTHEIMER AND JOSEPH E. MAYER
Department of Chemistry, University of Chicago, Chicago, Illinois

(Received August 2, 1946)

T. L. Hill has recently shown that it is possible to compute the magnitude of steric strain in certain organic molecules. The present paper summarizes the results of a similar but independent investigation directed towards a computation of the rate of racemization of optically active (i.e., sterically hindered) derivatives of diphenyl. The energy of the planar form of a sterically hindered diphenyl can be approximated by the equation:

$$E=\Sigma_i \tfrac{1}{2}a_i q_i^2+A_1 \exp(-d_1/\rho_1)+A_2 \exp(-d_2/\rho_2),$$

where the q_i are the normal coordinates of the unstrained molecule in question and the exponential terms are approximations (over the limited range of interest) to the steric repulsions of the non-bonded groups which repel each other. There are two such exponential terms, for in most sterically hindered diphenyls the repulsion is caused by two pairs of ortho substituents. The equation for E_0, the activation energy for racemization, has been found for the symmetrical case by minimizing E; the constants a_i, A, and ρ, and the dimensions of the diphenyl derivative appear in the expression for E_0. It is also possible to derive equations for the vibration frequencies of the planar form of the sterically hindered molecule (and, therefore, find the entropy of activation); these equations are complicated by the essential degeneracy of the vibrations in question.

I

IN a recent letter to the editor, T. L. Hill[1] has presented the outline of a general method for the quantitative (or at least semi-quantitative) evaluation of steric strain.[2] The method applies to those molecules where neighboring but non-bonded groups have been forced together so that they are separated by a distance less than the sum of their van der Waals radii. (An example of the type discussed by Hill is the addition compound of boron trifluoride and α, α'-lutidine, where the methyl groups in the base are forced close to the fluorine atoms in the boron derivative.[2b] Investigations by the same method as that suggested by Hill have been under way here for the past nine months, with special reference to the rate of racemization of optically active diphenyls. It seems therefore appropriate to supplement Hill's publication with those results obtained here which are of general applicability.

Hill suggested that the energy of a strained molecule is distributed among many bonds and is by no means concentrated in the energy of repulsion of the groups which have been pressed together. Quantitatively, Hill's equation is similar to Eq. (1), where E is the energy of the strained molecule in excess of that of a hypothetical molecule, identical in every way with the first, except that it has no steric strain.

$$E=\sum_i \tfrac{1}{2}a_i q_i^2+E(\text{steric}). \qquad (1)$$

Here E (steric) is a function of the distance d, between the groups or atoms which are involved in the steric interference. E(steric) may be negative (attraction) or positive (repulsion) but for most cases of interest, and certainly in the case studied here, it is positive. The variables q_i are coordinates which for the molecule in question are proportional to the displacements of all the atoms from their equilibrium positions. Equation (1) is written without cross-product terms, that is, without terms $a_{ij}q_iq_j$. The assumption is thus made that the coordinates, q_i, are mutually independent. This assumption is satisfied for the "normal" coordinates of the molecule but not in general for the increments (decrements) to the Cartesian coordinates of the various atoms. The sum in Eq. (1) must extend over all those coordinates, q_i, changes in which will affect the value of d. The force constant associated with each coordinate q_j is represented by a_j. The values of the coordinates, q_i, are to be

[1] T. L. Hill, J. Chem. Phys. **14**, 465 (1946). See also I. Dostrovsky, E. D. Hughes, and C. K. Ingold, J. Chem. Soc. 173 (1946).
[2a] R. Adams and H. C. Yuan, Chem. Rev. **12**, 261 (1933);
[2b] H. C. Brown, H. I. Schlesinger, and S. Z. Cardon, J. Am. Chem. Soc. **64**, 325 (1942).

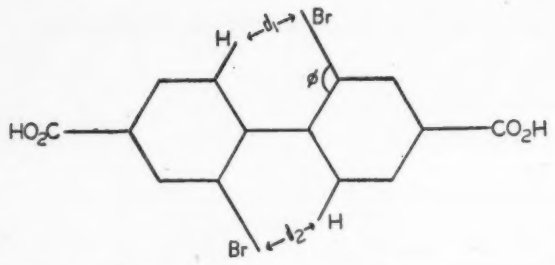

FIG. 1. Planar form (the activated complex) of the diphenyl.

chosen in such a way that E is a minimum. It should be noted that the larger the number of terms in Eq. (1) the lower will be the minimum value of E. This is the usual situation which obtains in a variation treatment, and is a necessary consequence of the fact that the energy depends upon a power of the displacement coordinates higher than the first.

II

The rest of this article is concerned with the quantitative treatment for the rate of racemization of optically active diphenyls such as 2,2′-dibromo-4, 4′-dicarboxydiphenyl.[3] The racemization of a compound of this type will occur only if the molecule passes through the planar configuration (Fig. 1). This will be the "activated complex" for the racemization of sterically hindered diphenyls.

It is worth noting in passing that the proposed treatment of steric strain assumes that the racemization involves (among other displacements) an increase in the angle, ϕ, between each ortho substituent and the benzene ring. This increase in angle will be sterically hindered by a substituent in the adjacent meta position. This conclusion is consistent with the experimental fact[4] that the rate of racemization of some diphenyl derivatives is uniformly and considerably decreased by substituents in this meta position. Substituents in other positions, although they affect the rate of racemization, do so to a much smaller extent, and they occasionally increase, rather than decrease, the racemization rate.

In the particular example chosen, only the hydrogen and bromine nuclei are close enough together to interfere strongly. (It is assumed that the bromine-bromine repulsions are so strong as to preclude the possibility of racemization through an activated complex in which these atoms are adjacent to one another.)The distance between a pair of hydrogen and bromine nuclei in the activated complex is represented by d; the distance between these nuclei which would obtain if there were no deviations from normal bond lengths and angles is called d_0. In the case under consideration, the energy of the two neighboring but non-bonded groups is predominately repulsive in character. It is convenient to approximate this repulsive energy by $A \exp(-d/\rho)$; this approximation should be valid for the values of d in question. The constants A and ρ can be evaluated by comparing the expression above with the energy curve computed from the second virial coefficient[5] for molecules which contain the same groups (here hydrogen and bromine) which repel each other in the activated complex.

In the case under discussion (2,2′-dibromo-4, 4′-dicarboxydiphenyl) each of the two bromine atoms must be forced close to a hydrogen atom in the activated complex. The repulsive energy for any distance, d, will then be twice that calculated from the energy curve to which reference has been made above. The same considerations will apply to other cases in which the diphenyl derivative is symmetrically substituted in the ortho positions. In the case of unsymmetrically substituted diphenyls, the sum of the repulsive energy for the two different sets of repelling groups would have to be used for E(steric) in Eq. (1). The energy of activation for the present case is that shown in Eq. (2):

$$E = \sum_i \tfrac{1}{2} a_i q_i^2 + 2A \exp(-d/\rho). \qquad (2)$$

Here the constants a_i are the force constants[6] associated with the normal coordinates q_i. Normal coordinates are chosen so that both the potential and kinetic energies involve only square and no cross-product terms. We wish to use such coordinates that the potential energy involves only squares but we are not primarily interested in the kinetic energy terms. It is

[3] W. I. Patterson and R. Adams, J. Am. Chem. Soc. **57**, 762 (1935).

[4] R. Adams and H. R. Snyder, J. Am. Chem. Soc. **60**, 1411 (1938).

[5] See, for example, O. K. Rice, J. Am. Chem. Soc. **63**, 3 (1941).

[6] For a discussion of these constants for benzene see E. Bernard, C. Manneback, and A. Verlaysen, Ann. Soc. Sci. Bruxelles **60**, 45 (1940); F. A. Miller and B. L. Crawford, J. Chem. Phys. **14**, 282 (1946).

therefore possible (except in Part III of this paper, in which the entropy of activation is discussed) to use bastardized coordinates which are not true normal coordinates but involve true normal coordinates of part of the molecule (the benzene rings) and force constants for other parts. In fact, the normal coordinates for the substituted diphenyls are not now available. However, the normal coordinates for benzene are known. In order to carry through the calculations, it will be necessary to assume that the force constants for the various deformations in each benzene ring are unaffected by the other aromatic nucleus. It will further be necessary to make some assumption about the magnitude of the force constant for the stretching vibration of the central carbon to carbon bond in the diphenyl derivative. The value of the activation energy computed on the basis of these assumptions should be the same as that which would be obtained from the normal coordinates of diphenyl provided only that a correct value for the stretching force constant of the central bond has been chosen. It should be noted, however, that the summation in (2) extends over all the normal coordinates in both benzene rings.

Preliminary calculations have shown that for diphenyls which racemize at measurable rates, only small changes in bond lengths and angles are necessary to attain the planar configuration. Because the displacement of each atom from its equilibrium position is small, it is possible as a good approximation to represent d as a linear function of the Cartesian displacement coordinates, x_i. Here, however, it will be necessary to set up separate functions for the distances d_1 and d_2 between the two hydrogen-bromine pairs, since the distances between the atoms in the two pairs are affected differently by changes in the various Cartesian displacement coordinates.

$$d_1=d_0+\sum_i l_i x_i, \quad d_2=d_0+\sum_i l_i' x_i. \tag{3}$$

There is a linear relationship[7] (Eq. (4)) between the Cartesian displacement coordinates of each atom and the normal coordinates, q_i.

$$x_j=\sum_i c_{ij} q_i. \tag{4}$$

(The normal coordinates of the benzene molecule, for example, are known in terms of the Cartesian displacement coordinates of each atom.[8]) Because of the considerations cited above, Eq. (3) may be written in the form (5)

$$d_1=d_0+\sum_i b_i q_i, \quad d_2=d_0+\sum_i b_i' q_i, \tag{5}$$

where

$$b_i=\sum_k l_k c_{ik} \quad \text{and} \quad b_i'=\sum_k l_k' c_{ik}. \tag{6}$$

The sum in Eq. (2) extends over all the normal coordinates, q_i. There will be some of these coordinates, however, changes in which do not change the internuclear distance, d; for example, this applies as a first approximation to the non-planar vibrations of the aromatic rings in a diphenyl derivative. For such a coordinate, q_k, the corresponding constant b_k is zero. It will be seen below (Eq. (10)) that when any particular b_i, say b_k, is zero, the value of q_k in the activated complex is also zero; the term in Eq. (2) involving this coordinate therefore contributes nothing to the energy, E, and may be omitted from the calculation if this for any reason seems desirable.

The combination of Eq. (2) and Eq. (5) leads to (7)

$$E=\sum_i \tfrac{1}{2} a_i q_i^2+E_{d_0} \exp\left[-(1/\rho)\sum_i b_i q_i\right]+E_{d_0} \exp\left[-(1/\rho)\sum_i b_i' q_i\right], \tag{7}$$

where $E_{d_0}=A \exp[(-d_0/\rho)]$. Here E_{d_0} is the repulsive potential which would have obtained if no bond lengths or angles had been distorted. It is now possible to find the minimum value for E; the values of the normal coordinates, q_i, in the activated state are represented by q_i^0

$$(\partial E/\partial q_j)=a_j q_j^0-(b_j/\rho)E_{d_0} \exp\left[-(1/\rho)\sum_i b_i q_i^0\right]-(b_j'/\rho)E_{d_0} \exp\left[-(1/\rho)\sum_i b_i' q_i^0\right]=0. \tag{8}$$

Let

$$E_{d_0} \exp\left[-\frac{1}{\rho}\sum_i b_i q_i^0\right]=E_{d_0} \exp\left[-\frac{1}{\rho}\sum_i b_i' q_i^0\right]=Z. \tag{9}$$

Since only definite values of the normal coordinates, corresponding to the "equilibrium" state of the

[7] Cf. G. Herzberg, *Infrared and Raman Spectra* (D. Van Nostrand Company, New York, 1945).
[8] E. B. Wilson, Phys. Rev. **45**, 706 (1934).

activated complex, occur in Z, it follows that Z itself is a constant for any particular optically active diphenyl. Further, from what has already been said about the constants b and b' and about the symmetry of the problem, it is clear that the two sums in Eq. (9) must be equal; this will also later be apparent from physical considerations. Then

$$q_j^0=\frac{(b_j+b_j')Z}{\rho a_j}=\frac{2B_jZ}{\rho a_j}, \tag{10}$$

where Eq. (10) defines B_j. Z can be obtained in terms of known constants by the numerical solution of Eq. (11), which equation results from the combination of (9) and (10).

$$Z=E_{d_0}\exp-[(2Z/\rho^2)\sum_i B_i^2/a_i]. \tag{11}$$

Substitution of the values of q_j^0 (Eq. (10)) into Eq. (7) yields E_0, the minimum value of E; E_0 is, therefore, the activation energy for racemization.

$$E_0=\sum_i \tfrac{1}{2}a_i(q_i^0)^2+2Z=\frac{2Z^2}{\rho^2}\sum_i\frac{B_i^2}{a_i}+2Z. \tag{12}$$

Z is therefore analogous to E(steric) of Eq. 1. It is the actual energy of repulsion of one pair of neighboring non-bonded groups in the activated state, and is of course much less than E_{d_0}. It is also clear that, for symmetrically substituted diphenyls, Z must be the same for the two halves of the molecule (i.e., Eq. (9) is valid).

Equation (12) for the energy of activation for the racemization of diphenyl derivatives is not precisely correct, since the resonance energy of the molecule has been neglected. However, the resonance energy for diphenyl itself, in excess of that for two benzene rings, amounts only to a few kilocalories[9]; the precise value of this energy term is, however, uncertain. When a satisfactory estimate of this resonance energy is available, the true activation energy can be found by subtracting the resonance energy from E_0. In the calculation of this latter quantity, the observed length of the carbon-carbon bond between the benzene rings in diphenyl should be used; this length is needed to evaluate the constants l_i and l_i', of Eq. (3).

However, until an accurate estimate of the resonance energy is available, an approximate method of calculation must be employed. The resonance in the planar form of diphenyl decreases the lengths of the carbon-carbon bond between the benzene rings. It follows, therefore, that the repulsion between the ortho substituents in the planar form of a sterically hindered diphenyl will be increased, because of resonance, over that which would have obtained in the absence of resonance.[10] This additional steric hindrance will diminish the absolute magnitude of the contribution of resonance to the energy of the planar configuration. Since the contribution of resonance even before it is diminished by steric effects, is small, the net effect on E_0 can probably be neglected.[11] It should be noted, however, that in any computation where resonance is neglected, the normal (i.e., aliphatic) carbon-carbon bond length should be used for the central bond in a diphenyl derivative.

Approximate numerical calculation of the activation energy for the racemization of 2,2′-dibromo-4,4′-dicarboxydiphenyl has led to a value of the order of 20 kcal.; a more refined calculation is in progress.

---

[9] G. W. Wheland, *The Theory of Resonance* (John Wiley and Sons, Inc., New York, 1944).

[10] M. Calvin, J. Org. Chem. 4, 256 (1939).

[11] The net effect, however, of resonance is to lower the energy of activation, E_0, although the amount by which E_0 is lowered is less than the resonance energy of diphenyl (in excess of that in the benzene rings). This conclusion follows because (a) resonance will be more important in the planar than in the non-planar structure of any diphenyl and (b) the energy of a resonance hybrid is always less (although perhaps only slightly less) than that predicted for the most stable individual structure which contributes to the ground state of the molecule in question. The stabilization of the activated complex by resonance, therefore, appears inevitable. The opposite viewpoint, which has previously (reference 10) been expressed, would appear to be in error.

III

The free energy of activation for racemization is given by the equation

$$\Delta F^* = E_0 - RT \ln (f^*/f), \tag{13}$$

where f^* is the partition function for the planar activated state and f the partition function for the non-planar normal state. The partition function for the normal state can be approximated by the product of partition functions, one for each vibrational and one for each rotational degree of freedom in the molecule; a similar statement applies to the activated complex. The partition functions depend, of course, on the vibration frequencies ν_i^* (of the activated complex) and ν_i (of the normal molecule). As a rough first approximation, each term in f^* will cancel the corresponding one in f. This approximate cancellation is the result in part of the fact that the vibration frequencies in the activated complex will not differ very much from those in the unstrained molecule. The cancellation is also the result in part of the fact that, for most of the vibrations in question, $h\nu_i$ is large compared with kT; the contribution of such a vibration to the entropy of activation will be small. An exception to the approximate cancellation of corresponding terms in the twisting vibration of the unstrained molecule about the central carbon-to-carbon bond in diphenyl, since this is the motion which, in molecules of high energy, leads to racemization.

Corresponding terms, however, do not precisely cancel since steric hindrance somewhat modifies the vibrational frequencies and energies on the activated complex. The energy of the activated complex is in fact represented by Eq. (14),

$$\begin{aligned} E &= \textstyle\sum_i \tfrac{1}{2} a_i (q_i^0 + q_i')^2 + E_{d_0} \exp\left[-(1/\rho) \sum_i b_i (q_i^0 + q_i')\right] + E_{d_0} \exp\left[-(1/\rho) \sum_i b_i' (q_i^0 + q_i')\right] \\ &= \textstyle\sum_i \tfrac{1}{2} a_i (q_i^0 + q_i')^2 + Z \exp\left[-(1/\rho) \sum_i b_i q_i'\right] + Z \exp\left[-(1/\rho) \sum_i b_i' q_i'\right], \end{aligned} \tag{14}$$

where the q_i' are small displacements from the "equilibrium" configuration of the activated complex, denoted by q_i^0. For sufficiently small values of the displacements, q_i', the exponential terms in (14) can be expanded in terms of the new coordinates, q_i'; this expansion together with Eqs. (10) and (12) lead to (15).

$$E - E_0 = \textstyle\sum_i \tfrac{1}{2} a_i (q_i')^2 + (Z/2\rho^2) \sum_i \sum_j (b_i b_j + b_i' b_j') q_i' q_j', \tag{15}$$

where the double summation is carried out over all values of i and j, including $i = j$. Whenever the potential energy, $E - E_0$, can be represented by a quadratic function of this sort, it is in principle[7] possible to eliminate the cross product terms $q_i' q_j'$. Further, if the coordinates q_i are true, normal coordinates, and if they have been normalized (i.e., if $T = \sum_i \dot{q}_i^2$), then the elimination of cross-product terms from Eq. (15) will lead to a new set of normal coordinates such that

$$E - E_0 = \textstyle\sum_i \alpha_i Q_i^2 \tag{16}$$

and

$$T = \textstyle\sum_i \dot{Q}_i^2. \tag{16'}$$

The frequencies of vibration for the activated complex are related to the new force constants α_i, by the expression

$$\alpha_i = 4\pi^2 \nu_i^{*2} \tag{17}$$

just as the vibration frequencies of the unstrained (non-planar) molecule are related to the corresponding force constants a_i by the expression

$$a_i = 4\pi^2 \nu_i^2. \tag{17'}$$

The general transformation of (15) to (16) demands the solution of a secular equation with n roots, where n is the number of vibrational degrees of freedom of the molecule in question. The solution of such an equation, in the general case, is very difficult, and in many cases cannot reasonably be performed. However, in the event that the cross-product terms in (15) are small compared to the terms $a_i (q_i')^2$, the secular equation can be solved by perturbation methods. The actual solution leads to expressions for the force constants α_i, the frequencies of vibration ν_i^*, of the activated state, and finally by way

of Eq. (13) to the free energy of activation and the absolute rate of reaction. Unfortunately, the perturbation method is considerably complicated by the essential degeneracy of many of the benzenoid vibrations. Since for the cases under consideration the two benzene rings are identically substituted, every vibration of the diphenyl molecule is at least doubly degenerate and those corresponding to the doubly degenerate levels of the benzene ring are fourfold degenerate. In principle, these degeneracies can be eliminated, and the perturbation method can be carried through to completion. However, since the steps necessary to this solution are concerned with the details of the particular example chosen, it seems best to postpone the presentation of the explicit solution of this case. The authors hope soon to carry out numerical calculations based on this development.

IV

Although the present treatment has been restricted to a consideration of the racemization of diphenyls, it is clearly of much broader application. An equation analogous to (12) will predict the energy of reaction for those cases in which an equilibrium constant rather than a rate constant can be observed.

V

The authors wish to thank Dr. G. W. Wheland for his valuable advice and assistance in this research.

THE JOURNAL OF CHEMICAL PHYSICS VOLUME 14, NUMBER 12 DECEMBER, 1946

On the Equation of State for Gases at Extremely High Pressure

P. CALDIROLA
Istituto di Fisica, Università di Pavia, Pavia, Italy
(Received July 18, 1946)

On the basis of the thermo-hydrodynamic theory of the explosive detonation—developed by Chapman, Jouguet, and R. Becker—a procedure is developed permitting the deduction of the equation of state for gaseous mixtures from explosive processes. The equation is established by starting from several sets of experimental data. In this way one can semi-empirically derive the equation of state for gases compressed up to 10^4–10^5 atmos. The results of numerical calculations are reported.

I

DIRECT experimental measurements allow one to derive the equation of state for gases up to pressures of some thousand atmospheres. But we have little knowledge about the properties of gases compressed up to 10^4–10^5 atmos.; this is the order of the instantaneous pressures of gaseous products resulting from the detonation of solid explosives. Therefore, the fundamental importance, from the chemical-physical viewpoint, presented by the knowledge of the properties of gases at these particular conditions is evident.

The purpose of this work is in the first place to show that, when one admits the validity of the thermo-hydrodynamic theory of detonation as developed by Chapman,[1] Jouguet,[2] and R. Becker,[3] and makes use of a few experimental data, then one can determine the equation of state for gases applicable during the detonation: the pressures of these gases can be of the order of 10^5 atmos.

In order to make more comprehensible our

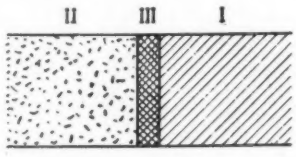

FIG. 1. Explosion process.

[1] D. L. Chapman, Phil. Mag. **47**, 90 (1899).
[2] Jouguet, J. de Math. **1**, 347 (1905); **2**, 6 (1906).
[3] R. Becker, Zeits. f. Physik **8**, 321 (1922).

procedure, we will sketch briefly the thermo-hydrodynamic theory of the explosion. Let us consider, for this purpose, Fig. 1, which represents, at a certain instant, the state of the system composed of the unexploded substance, and the products obtained in the detonation, when the explosive reaction takes place in a cylindrical container with indeformable walls. The part of the container on the right I is filled with the unexploded substance (gas, liquid, or solid), the part on the left II is filled by the mixture of the explosion products, and the intermediate part III represents the zone (whose depth, following Becker, is about 10^{-7} cm), where the explosive transformation takes place. Let us denote by D the velocity with which this zone (wave front) proceeds (velocity of detonation), and W the velocity of the gaseous explosion products; let us denote by ρ_1, T_1, p_1 and by ρ, T, p the density, the temperature, the pressure, respectively, of the unexploded substance and of the gaseous products.

In the steady conditions ($D=$const.), and assuming that the effect of heat losses is negligible, the principles of continuity of mass, conservation of energy, and momentum, then, provide the following equations:

$$\rho_1 D=\rho(D-W), \tag{1}$$

$$p_1 D+\rho_1 D\left(E_1+\frac{D^2}{2}\right)$$

$$=p(D-W)+\rho(D-W)\left[E+\frac{(D-W)^2}{2}\right], \tag{2}$$

$$p_1+\rho_1 D^2=p+\rho(D-W)^2 \tag{3}$$

(E_1 and E denote the specific internal energy of two phases).

To the preceding equations, which are hydrodynamical in nature, we shall now add the thermodynamic relation:

$$E-E_1=\int_{T_1}^{T} c_v dT-q=\bar{c}_v(T-T_1)-q, \tag{4}$$

and the equation of state for the gases of the mixture resulting from explosion:

$$F(\rho, p, T)=0. \tag{5}$$

It can easily be shown that Eqs. (1)–(5) permit one to obtain D, W, T as functions of the parameters p, ρ and of the characteristics of the unexploded substance:

$$D=\left[\frac{p-p_1}{\rho-\rho_1}\frac{\rho}{\rho_1}\right]^{\frac{1}{2}}, \tag{6}$$

$$W=\left[(p-p_1)\frac{\rho-\rho_1}{\rho\rho_1}\right]^{\frac{1}{2}}, \tag{7}$$

$$T=\varphi(\rho, p). \tag{8}$$

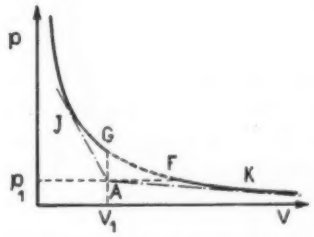

FIG. 2. Hugoniot's curve for an explosion process.

Moreover, one arrives at a relation between p and v (where $v=1/\rho$ is the specific volume of the gaseous mixture):

$$\bar{c}_v[\varphi(p, v)-T_1]-q=\tfrac{1}{2}(p_1+p)(v_1-v). \tag{9}$$

This relation is represented on the (V, p) diagram (Fig. 2) by a curve known as Hugoniot's curve or H curve. This gives us all the infinite states of the gaseous mixture, which are *a priori* possible. In the H curve we can distinguish three parts: the first is formed from the complex of points above the point G, the second from the complex of points between G and F, and the third from the complex of points under F. As one can immediately verify with the aid of relations (6), (7), corresponding to the first part of the H curve (detonation) $D>W>0$; corresponding to the second part (which represents no physical transformation) D and W assume imaginary values; and last, corresponding to the third part (deflagration) $D>0$ and $W<0$.

Further, making use of several considerations about the entropy of the system, one can prove (see for example Schorah[4]) that there exists only one point of the H curve to which corresponds a stable state of the detonation process. This state is analytically determined by the fact that, corresponding to it, the derivative dS/dv of the entropy must be taken equal to zero; graphically

[4] R. L. Schorah, J. Chem. Phys. **3**, 425 (1935).

the stable state is represented by the contact point of the tangent to the curve H from the point (v_1, p_1), characteristic of the state of the unexploded substance. The fact that, corresponding to the stable state, we have

$$D=U+W$$

is of considerable importance, where U denotes the velocity of sound in the mixture of gases resulting from detonation.

2

If we take the equation of state (5) to be known, it is possible to calculate all the quantities ρ, p, T, D, W which characterize, from the physical standpoint, any gaseous explosive, because the pressure of gases deriving from the detonation reaches some thousand atmospheres: the results of theoretical calculations—see for example Lewis[5]—are in very reasonable agreement with experimental facts. On the other hand, in the detonation of solid explosives gaseous mixtures are produced whose pressures can reach above 10^5 atmos. In theoretical calculations one experiences the difficulty that at such extremely high pressures no experimentally proved equation of state is known. In this connection, we shall now show that if we start from the experimental relation between the velocity of detonation D and the density of the unexploded substance ρ_1, not only can we unequivocally derive the values of the further explosion parameters (W, ρ, p, T) without *a priori* knowledge of the equation of state for the gaseous products, but we can also arrive at such an equation. Writing the unknown equation of state in the very general form

$$pv=r(v)T, \tag{10}$$

we see indeed that the H curve of the detonation process obeys the equation $(p_1 \ll p)$

$$p=\frac{A}{B(v)v-\frac{1}{2}v_1},$$

where

$$A=\bar{c}_v T_1+q, \quad B(v)=\frac{\bar{c}_v}{r(v)}+\frac{1}{2}.$$

The stable state, which can be obtained—as we have remarked—by the determination of the contact point of the tangent to the H curve from the initial point (v_1, p_1), is in this case determined by the equation in η:

$$\eta^2+2k\eta-(k-\sigma)=0, \tag{11}$$

where

$$\eta=\frac{W}{D}, \quad k=\frac{2A}{D^2}, \quad \sigma=\tfrac{1}{2}\eta(1-\eta)v_1\frac{(dB/dv)}{B}(k+\eta).$$

σ being very small with respect to k, we can easily solve Eq. (11) following a method of successive approximations.

From the values of η, which we obtain in this way, we derive further the corresponding values

TABLE I. Nitropentaerytrite.

ρ_1 (kg/dm³)	D (m/sec.)	ρ (kg/dm³)	p (kg/cm²)	T (°K)
0.5	3960	0.79	29,600	4670
0.65	4400	1.00	44,900	4840
0.8	4900	1.20	65,000	5050
1.0	5500	1.45	95,300	5320
1.2	6300	1.69	140,500	5720
1.4	7100	1.93	195,500	6170
1.6	7900	2.15	262,800	6670

TABLE II. Tetryl.

ρ_1 (kg/dm³)	D (m/sec.)	ρ (kg/dm³)	p (kg/cm²)	T (°K)
1.00	5480	1.43	91,800	4400
1.28	6510	1.80	160,400	4740
1.45	7220	2.02	218,100	4980
1.54	7375	2.15	242,500	5100
1.61	7470	2.20	259,100	5140

[5] Lewis, Chem. Rev. 10, 49 (1932).

TABLE III. Picric acid.

ρ_1 (kg/dm³)	D (m/sec.)	ρ (kg/dm³)	p (kg/cm²)	T (°K)
1.03	5150	1.47	83,000	3880
1.23	5820	1.72	120,700	4070
1.39	6450	1.93	164,600	4280
1.63	7210	2.25	239,400	4660

TABLE IV. Trinitrotoluene.

ρ_1 (kg/dm³)	D (m/sec.)	ρ (kg/dm³)	p (kg/cm²)	T (°K)
1.0	4700	1.44	68,700	3210
1.29	5900	1.82	132,800	3610
1.46	6500	2.04	178,000	3860
1.59	6900	2.22	216,200	4020

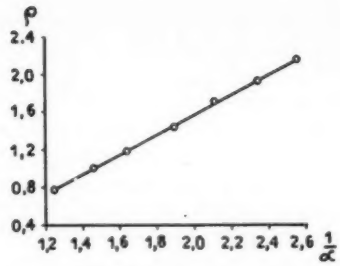

FIG. 3. Equation of state for detonation gases: nitropentaerytrite.

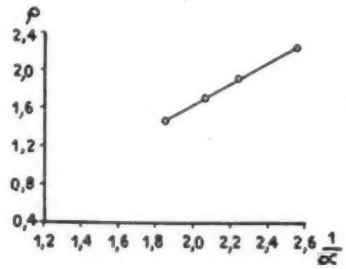

FIG. 4. Equation of state for detonation gases: tetryl.

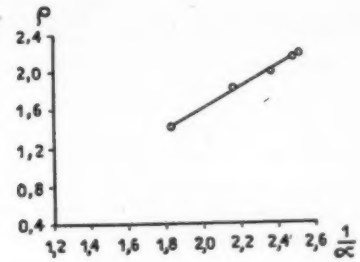

FIG. 5. Equation of state for detonation gases: picric acid.

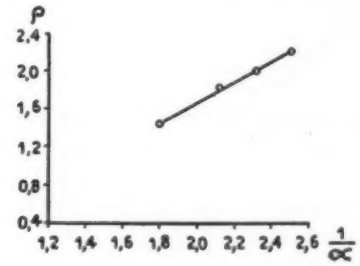

FIG. 6. Equation of state for detonation gases: trinitrotoluene.

of ρ, p, T making use of Eqs. (6)–(8). Following this procedure we have the possibility of establishing the function $r(v)$ and therefore the unknown equation of state.

We have performed numerical computations for several explosives (nitropentaerytrite, tetryl, picric acid, trinitrotoluene) assuming as starting point the experimental relation between the detonation velocity D and the density of explosive, derived from the results of careful measurements performed by Friederich.[6] For the chemical equations of the explosive reactions, characteristic of the detonation processes, we have taken the data from A. Schmidt[7]; the values of the mean specific heats as functions of the temperature, for every gaseous mixture were calculated starting from the data contained in Beyling-Drekopf's book.[8]

Tables I–IV present a summary of the results of our numerical calculations.

From our results we can conclude that the quantities p, v, T of the gaseous mixtures resulting from the several processes of detonation are in good accordance with the equation (due to Van Laar)

$$p[v-\alpha(v)]=nRT, \tag{12}$$

with

$$\alpha(v)=\frac{b}{1+c/v}=\frac{b}{1+c\rho}, \tag{13}$$

where the constants b, c have the following numerical values:

nitropentaerytrite:	$b=2.08$	$c=2.00$
tetryl:	$b=1.81$	$c=1.62$
picric acid:	$b=1.96$	$c=1.79$
trinitrotoluene:	$b=2.07$	$c=1.88$

In order to illustrate the accuracy with which the equation of state (12) is verified, we have plotted in Figs. 3–6 the values of ρ against the values of $1/\alpha$ for the gaseous mixture of the explosives considered. One can see that the dependence is really linear, as one must expect from Eq. (13).

Finally, attention is called to the fact that the equation of state (12), which we have derived, is suitable only within the range of pressures and temperatures occurring in processes of detonation of solid explosives, that is approximatively from 30,000 to 300,000 atmos., and from 3000 to 7000°K.

[6] W. Friederich, Zeits. ges. Schiess. und Sprengstoffe **28**, 2, 51, 80, 143, 213, 244 (1933).
[7] A. Schmidt, Zeits. ges. Schiess. und Sprengstoffe **33**, 364 (1938); **34**, 8, 37, 80 (1939).
[8] C. Beyling and K. Drekopf, *Sprengstoffe und Zündmittel* (Julius Springer, Berlin, 1936).

Letters to the Editor

THIS section will accept reports of new work, provided these are terse and contain few figures, and especially few halftone cuts. The Editorial Board will not hold itself responsible for opinions expressed by the correspondents. Contributions to this section should not exceed 600 words in length and must reach the office of the Managing Editor not later than the 15th of the month preceding that of the issue in which the letter is to appear. No proof will be sent to the authors. The usual publication charge ($3.00 per page) will not be made and no reprints will be furnished free.

The Critical Micelle Concentration of Anionic Soap Mixtures

H. B. KLEVENS*
Department of Chemistry, University of Chicago, Chicago, Illinois
September 5, 1946

MANY technical papers have dealt with the increase in solubilization, wetting, detergency, etc., of soap mixtures as compared with pure soaps, but except for some ultramicroscopic studies there have been no data reported on the properties of soap mixtures in the region of the critical micelle concentration (*cmc*). The changes occurring in dye spectra upon the addition of varying amounts of soaps[1] have been used in this work.

The change in *cmc* (the sum of the concentration of the two soaps) of soap mixtures (potassium myristate plus potassium laurate, potassium caprate, potassium caprylate, and sodium lauryl sulfate) as determined with the dye, pinacyanol chloride, is plotted in Fig. 1. The *cmc* of potassium caprylate and potassium caprate have not been reported previously by means of the dye method, but the values of 3.94×10^{-1} and 9.9×10^{-2} *M* observed here agree with those of 3.6–3.8×10^{-1} and 9.5–10.0×10^{-2} reported by Ekwall,[2] and 3.7–4.0×10^{-1} and 10.0–10.2×10^{-2} as determined by refraction.[3] Other unreported data which will be discussed in a following report include mixtures of alkyl sulfonates as well as potassium laurate plus potassium caprate and potassium caprylate, and potassium caprate plus potassium caprylate. Similar results have been observed for mixtures of cationic soaps using indophenol[4] as the dye indicator.

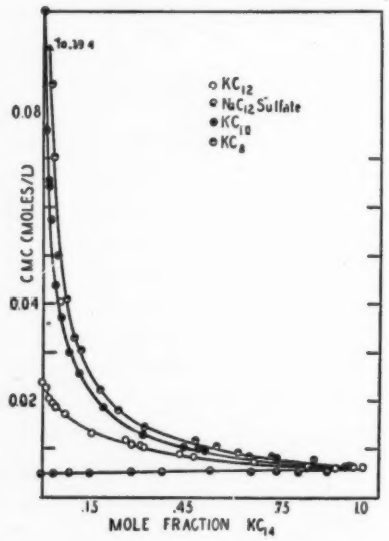

FIG. 1. The critical micelle concentrations in moles per liter (the sum of the concentrations at the appearance of micelles) of various soap mixtures.

It can be seen from the curves in Fig. 1 that the greatest change in *cmc* of the soap mixtures is observed when there is the largest difference in the *cmc* of the pure soaps. It is also evident that there are no *cmc* values which do not fall within the range of values of the pure soaps. These results over certain mole fraction ranges are similar to the effects of salts on the *cmc* of pure soaps.[5] In this connection, however, it is necessary to consider not the sum of the concentration in the soap mixture at the appearance of micelles, but the concentration of one of the soaps at this point as affected by the other. When this is done, it is found, for example, that potassium caprate acts like a salt, say potassium chloride or sodium chloride, depressing the necessary concentration of potassium laurate. This value, which is equal to the mole fraction times the total *cmc*, is found to be similar to a salt effect for mole fractions of the laurate as low as 0.50.

This treatment was found to be valid in various other mixtures only in the region of higher mole fractions of the less soluble soap. In the portion of the curves in Fig. 1 where the greatest change in the total *cmc* occurs, the salt effect phenomena were not observed. Thus, a much greater change in the total *cmc* can be obtained by adding a small amount of a less soluble soap than by adding an equivalent amount of a salt. The tendency of the less soluble soap to aggregate seems to have a much greater effect on the total aggregation associated with micelle formation than a salt.

When two soaps of approximately the same *cmc* are mixed, there is no observable change in the *cmc* of the mixture and no region of a salt effect is observed. A mixture of this type, potassium myristate plus sodium lauryl sulfate, is seen in Fig. 1.

In the consideration of soap mixtures, it seems that the difference in the tendency of single soaps to form micelles controls the micelle formation in their mixtures; the greater the difference (for example in solubility), the greater will be the initial effect of the more soluble soap. If this tendency to aggregate is different in two soaps, then in a limited concentration range of mixtures, the soap having the lower tendency to aggregate will act as a salt towards the other. Soaps having about the same tendency to aggregate will have little effect on each other as far as salt effect and change in total *cmc* are concerned.

* Present address: Chemical & Physical Research Laboratories Firestone Tire & Rubber Company, Akron, Ohio.
[1] M. L. Corrin, H. B. Klevens, and W. D. Harkins, J. Chem. Phys. **14**, 480 (1946).
[2] P. Ekwall, Kolloid Zeits. **101**, 135 (1942).
[3] H. B. Klevens, J. Chem. Phys. **14**, 567 (1946).
[4] H. B. Klevens, J. Am. Chem. Soc. to be published.
[5] M. L. Corrin and W. D. Harkins, in preparation.

A Relation Between Bond Multiplicity and Interatomic Distance

R. T. LAGEMANN
Emory University, Emory University, Georgia
November 14, 1946

IN a note bearing the above title, Kavanau[1] has advanced a most useful relation connecting the interatomic distances of covalent bonds to the bond multiplicity. He suggests that

$$D=a+b\left(\frac{n_1+n_2-1}{n_1+n_2+1}\right)^N, \qquad (1)$$

where D is the interatomic distance in angstroms; a and b are constants determined by the specific atom pair; N is the bond multiplicity; and n_1 and n_2 are the principal quantum numbers of the valence electrons in the bonded atoms.

Examination of the constants a and b given by Kavanau shows them to be roughly related to the sum Z of the atomic numbers of the atoms making up the bonded pair. If we set b proportional to Z and a inversely proportional to Z, we have

$$D=\frac{K_1}{Z}+K_2Z\left(\frac{n_1+n_2-1}{n_1+n_2+1}\right)^N, \qquad (2)$$

TABLE 1. Observed and calculated bond lengths.

Molecule	Atom pair	Bond order	Bond length in A D obs.	Bond length in A D calc.	Percent deviation
C_2H_6	CC	1.11	1.55[c]	1.50	3.2
CH_3CCH	CC	1.23	1.46[c]	1.47	0.7
C_6H_6	CC	1.78	1.39[c]	1.36	2.2
C_2H_4	CC	2.12	1.33[c]	1.31	1.5
CH_3CCH	CC	2.89	1.21[c]	1.22	0.8
C_2H_2	CC	3.00	1.204[a]	1.21	0.8
CH_3F	CF	1.00	1.396[a]	1.44	2.9
CH_3NH_2	CN	1.00	1.47[a]	1.49	1.4
HCN	CN	3.00	1.154[a]	1.15	0.0
CH_3OH	CO	1.00	1.43[a]	1.46	2.1
H_2CO	CO	2.00	1.21[a]	1.23	1.7
F_2	FF	1.00	1.435[a]	1.42	1.4
NH_2NH_2	NN	1.00	1.47[b]	1.46	0.7
$(C_6H_5N)_2$	NN	2.00	1.23[b]	1.23	0.0
N_2	NN	3.00	1.095[a]	1.09	1.0
OF_2	OF	1.00	1.41[a]	1.42	0.7
			Average percent deviation		1.3

[a] W. Gordy, J. Chem. Phys. **14**, 305 (1946).
[b] J. L. Kavanau, J. Chem. Phys. **12**, 467 (1944).
[c] R. S. Mulliken, C. A. Rieke, and W. G. Brown, J. Am. Chem. Soc. **63**, 41 (1941).

where K_1 and K_2 are considered constant for all pairs of atoms having the same value of n_1 and the same value of n_2. This modification covers more cases with two constants than does Kavanau's original relation, and seems to have considerable merit in empirically correlating bond length and multiplicity. Figure 1 shows the linearity of *DZ versus* $Z^2\,(3/5)^N$ for pairs of atoms for which $n_1=n_2=2$.

Table I gives a list of atom pairs whose valence electrons

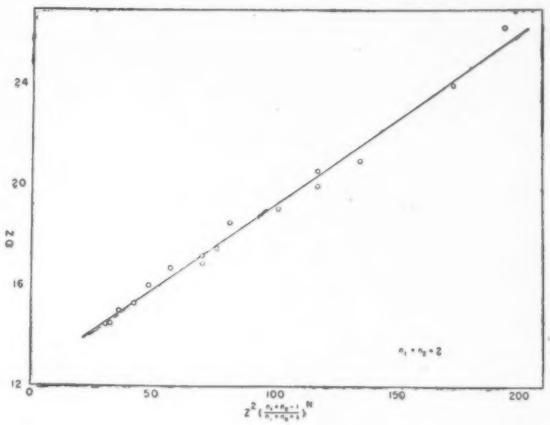

FIG. 1.

possess principal quantum numbers of 2. Included in the table are values of the observed interatomic distances and values of the interatomic distance calculated from Eq. (2) using $K_1=12.45$, and $K_2=0.0676$. The values of K_1 and K_2 were obtained by a least squares treatment of the experimental bond lengths. The combination $n_1=n_2=2$ was selected at random for presentation here, but other combinations of the principal quantum numbers appear on preliminary inspection to yield similar results.

It will be noted that the proposed relation holds for isotopic molecules where Z and D are constant. However, it does not care in a precise way for cases such as CO and N_2 where Z is the same for both molecules but the observed interatomic distance is clearly not.

[1] J. L. Kavanau, J. Chem. Phys. **12**, 467 (1944).

THE AMERICAN INSTITUTE OF PHYSICS

INCORPORATED

57 East 55 Street New York 22, N.Y.

MEMBER SOCIETIES:

American Physical Society
KARL K. DARROW, *Secretary*, Columbia University, New York 27, New York.

Optical Society of America
ARTHUR C. HARDY, *Secretary*, Massachusetts Institute of Technology, Cambridge 39, Massachusetts.

Acoustical Society of America
WALLACE WATERFALL, *Secretary*, 350 Fifth Avenue, 64th floor, New York 1, New York.

Society of Rheology
R. B. DOW, *Secretary*, Bureau of Ordnance, Navy Department, Washington 25, D. C.

American Association of Physics Teachers
C. J. OVERBECK, *Secretary*, Northwestern University, Evanston, Illinois.

ASSOCIATED SOCIETIES:

American Society for X-Ray and Electron Diffraction

Electron Microscope Society of America

Physical Society of Pittsburgh

Physics Club of Chicago

Physics Club of Philadelphia

ASSOCIATES:

Over seventy-five leading industrial enterprises and other institutions which contribute to the support of the Institute.

JOURNALS:

The Physical Review
Reviews of Modern Physics
JOHN T. TATE, *Editor*—J. W. BUCHTA, *Assistant Editor*

Journal of the Optical Society of America
GEORGE R. HARRISON, *Editor*

The Journal of the Acoustical Society of America
FLOYD A. FIRESTONE, *Editor*

American Journal of Physics
DUANE ROLLER, *Editor*—JOSEPH D. ELDER, *Assistant Editor*

The Review of Scientific Instruments
GAYLORD P. HARNWELL, *Editor*

The Journal of Chemical Physics
JOSEPH E. MAYER, *Editor*

Journal of Applied Physics
ELMER HUTCHISSON, *Editor*

OFFICERS

PAUL E. KLOPSTEG, *Chairman*
Northwestern University

WALLACE WATERFALL, *Secretary*
The Celotex Corporation

GEORGE B. PEGRAM, *Treasurer*
Columbia University

JOHN T. TATE,
Adviser on Publications
University of Minnesota

COVERNING BOARD

R. B. DOW
L. A. DUBRIDGE
W. F. FAIR, JR.
FLOYD A. FIRESTONE
HARVEY FLETCHER
R. C. GIBBS
K. S. GIBSON
PAUL E. KLOPSTEG
W. H. MARKWOOD, JR.
GEORGE B. PEGRAM
A. H. PFUND
JOHN T. TATE
L. W. TAYLOR
WALLACE WATERFALL
A. G. WORTHING

ADMINISTRATIVE STAFF

HENRY A. BARTON, *Director*

MARGARET S. GRIFFIN,
Publications Manager

THEODORE VORBURGER,
Business Manager

THE American Institute of Physics was founded in 1931 as a federation of leading societies in the field of Physics. It combines into one operating agency those functions on behalf of physics which can best be done by the Societies jointly. Its purpose is the advancement and diffusion of physics and its applications to human welfare. To this end it publishes for itself or the Societies the eight journals listed on this page; promotes unity and effectiveness of effort among all who are interested in physics; renders numerous direct services to physicists and to the public; and cooperates with government agencies, national associations, educational institutions, technical industries, and others in such manner as to realize the opportunities and fulfill the responsibilities of physics as an important and constructive human activity.

CONTENTS

THE JOURNAL OF CHEMICAL PHYSICS VOL. 14, NO. 12 DECEMBER, 1946

Mass Spectrometric Study of CH_3D. Dissociation Probabilities of C—H and C—D Bonds by Electron Impact . . . . . MARJORIE W. EVANS, NORMAN BAUER, AND J. Y. BEACH 701

Mercury Photo-Sensitized Reaction Between Hydrogen and Oxygen . . . DAVID H. VOLMAN 707

Investigation of Oxidation of Copper by Use of Radioactive Cu Tracer . . . . . J. BARDEEN, W. H. BRATTAIN, AND W. SHOCKLEY 714

Proposed Interpretation of the Zeta-Potential . . . . . LAWRENCE B. ROBINSON 721

Absorption of Water by Films of Cellophane and Polyvinyl Alcohol . . . . . E. CREUTZ AND ROBERT R. WILSON 725

Thermodynamic Properties of Gaseous Boron Triflouride, Boron Trichloride, and Boron Tribromide . . . . . HUGH M. SPENCER 729

Theory of the Racemization of Optically Active Derivatives of Diphenyl . . . . . F. H. WESTHEIMER AND JOSEPH E. MAYER 733

On the Equation of State for Gases at Extremely High Pressure . . . . . P. CALDIROLA 738

Letters to the Editor:

Critical Micelle Concentration of Anionic Soap Mixtures . . . . . H. B. KLEVENS 742

Relation Between Bond Multiplicity and Interatomic Distance . . . . . R. T. LAGEMANN 743

Author Index to Volume 14 744

Analytic Subject Index to Volume 14 748

Volume Table of Contents iii

LANCASTER PRESS, INC., LANCASTER, PA.